Master's thesis

NTNU
Norwegian University of Science and Technology
Faculty of Information Technology and Electrical Engineering
Department of Electric Power Engineering

Margrete Haaland

Stability limits for optimal power flow related to congestion management

Master's thesis in Energy and Environmental Engineering
Supervisor: Kjetil Uhlen
June 2020

NTNU
Norwegian University of Science and Technology

Margrete Haaland

Stability limits for optimal power flow related to congestion management

Master's thesis in Energy and Environmental Engineering
Supervisor: Kjetil Uhlen
June 2020

Norwegian University of Science and Technology
Faculty of Information Technology and Electrical Engineering
Department of Electric Power Engineering

NTNU
Norwegian University of
Science and Technology

Abstract

The aim of this thesis is to perform dynamic simulations of a 4-bus model and an aggregated model of the Nordic power system (N44) to decide the transmission constraints of selected lines. The transmission constraints will be used when the optimal power flow is simulated to investigate how the constraints affects the operating costs. For the N44 model the optimal power flow was simulated after a contingency to investigate the redispatch and change in operating costs for different transmission constraints.

A great amount of the vital services in today's society is dependant of electricity, making the power system an essential infrastructure. Congestion, and other challenges, becomes more common when the power system is upgraded with renewable energy and digital solutions. In addition, the power demand increases faster than the power system is upgraded, making it crucial to utilize the power system optimally. The security rating of the transmission lines are not common to use when the transmission constraints are decided. The security rating is decided by the stability of the system. In this thesis, the stability of the systems is investigated through dynamic simulations, with focus on voltage stability and rotor angle stability, to determine the security rating of selected lines.

The models that were analyzed in this thesis was a 4-bus model with two generators and two loads, and the N44 model of the Nordic power system. The dynamic simulations focused on a contingency of a specific line in both models. For the 4-bus model, the focus was on one of the lines connecting a generator and a load. For the N44 model, the focus was on one of the lines connecting Eastern Norway to Sweden. The dynamic analysis included voltage stability analysis and rotor angle stability analysis, and was performed for different operating states for both models.

The power system optimization was performed in MATPOWER in MATLAB®. The simulations were performed on equivalent models to analyze how the objective function value, and the redispatch after a contingency, was affected by the transmission constraint.

The results showed that the voltage stability was the limiting factor, and that the transmission constraints did not affect the OPF solution for the 4-bus model. For the N44 model, the rotor angle stability, with damping and critical clearing time, was the limiting factor. A few values of the transmission constraint were proposed, where the transmission constraint of max. 2200 MW was suggested to ensure a damping ratio above 0.03 and a critical clearing time above 150 ms. It was also discovered that the tranmsission constraint play an important part in the OPF solution of the N44 model, as the operating costs increased with a decreased transmission constraint. The constraint of 2200 MW corresponds to an increase in operating costs of 25 000 $\$/hr$.

In further work, it would be interesting to perform more extensive analysis on the N44 model including contingencies on more lines. It it also of interest to integrate reliability analysis with the OPF analysis to find an optimum between operating and interuption costs.

Sammendrag

Målet for denne masteroppgaven er å utføre dynamiske simuleringer på en enkel modell med fire samleskinner samt en forenklet modell av det nordiske kraftsystemet (N44) for å bestemme overføringsgrensene for utvalgte linjer. Overføringsgrensene vil bli brukt når den optimale lastflyten blir simulert for å undersøke hvordan begrensningene påvirker driftskostnadene. For N44-modellen ble den optimale lastflyten simulert etter et utfall for å undersøke den optimale bruken av resever og hvordan driftskostnader endres for forskjellige overføringsgrenser.

En stor del av de viktigste tjenestene i dagens samfunn er avhengig av strøm, noe som gjør kraftsystemet til en viktig infrastruktur. Overbelastning, og andre utfordringer, blir mer vanlig når kraftsystemet blir oppgradert med fornybar energi og digitale løsninger. Når strømbehovet i tillegg øker raskere enn kraftsystemet blir oppgradert, er det avgjørende å utnytte kraftsystemet optimalt. Stabilitetsgrensene til overføringslinjene er ikke vanlig å bruke når overføringsgrense bestemmes. I denne oppgaven blir stabilitet undersøkt gjennom dynamiske simuleringer, med fokus på spenningsstabilitet og vinkelstabilitet, for å bestemme stabilitetsgrensene til utvalgte linjer.

Modellene som ble analysert i denne oppgaven var en enkel modell med to generatorer og to laster, og N44-modellen av det nordiske kraftsystemet. De dynamiske simuleringene fokuserte på et utfall av en spesifikk linje i begge modellene. For den enkle modellen var fokuset på en av linjene som forbinder en generator og en last. For N44-modellen var fokuset på en av linjene som forbinder Øst-Norge med Sverige. Den dynamiske analysen inkluderte spenningsstabilitetsanalyse og vinkelstabilitetsanalyse, og ble utført for forskjellige driftstilstander for begge modellene.

Den optimale lastflyten ble utført i MATPOWER i MATLAB®. Simuleringene ble utført på ekvivalente modeller for å analysere hvordan verdien til objektivfunksjonen, og den optimale bruken av reserver etter et utfall, ble påvirket av overføringsgrensene.

Resultatene viste at spenningsstabiliteten var den begrensende faktoren, og at overføringsgrensene ikke påvirket OPF-løsningen for den enkle modellen. For N44-modellen var vinkelstabiliteten den begrensende faktoren. Videre ble det foreslått noen verdier for overføringsgrensen, der en overføringsgrense på maks. 2200 MW skulle sikre akseptable forhold. Det ble også oppdaget at overføringsgrensen spiller en viktig rolle i OPF-løsningen for N44-modellen, ettersom driftskostnadene økte med redusert overføringsgrense. Grensen på 2200 MW tilsvarer en økning i driftskostnadene på 25 000 $\$/hr$.

I videre arbeid vil det være interessant å utføre en mer omfattende analyse av N44-modellen, inkludert utfall på flere linjer. Det er også av interesse å integrere

pålitelighetsanalyse med OPF for å finne et optimum mellom drifts- og avbruddskostnader.

Preface

This thesis is the final work of the M.Sc. programme Energy and Environmental Engineering at the Department of Electric Power Engineering at Norwegian University of Science and Technology. It is credited 30 ECTS points and is written in collaboration with SINTEF Energy Research. This thesis is a continuation of my previous work in my specialization project written in the previous semester. For that reason, most of the literature research was carried out during the fall of 2019. The work done this spring has not been quite as expected as NTNU closed in March due to the COVID-19 pandemic. I have therefore done a lot of the work from home with digital guidance.

I would like to thank my supervisor Kjetil Uhlen for guidance and support throughout the semester. I would also like to thank my co-supervisor at SINTEF Energy Research, Sigurd Hofsmo Jakobsen, for always having an open door and being available for questions and guidance. At last, I would like to thank all my friends and fellow students at NTNU, who have helped me through discussions and by always being supportive.

Trondheim, June 9, 2020

Margrete Haaland

Table of Contents

List of Figures

List of Tables

1 Introduction

1.1 Background and motivation

The power system is an essential infrastructure in every modern society [13], as most of the vital services are dependant on electricity [12]. The increase in renewable energy, digital solutions, and more connections to the European power system creates more vulnerable power system with several new challenges and threats [40]. Congestion, for instance, become more common in systems with rapid deployment of renewable energy sources [6]. Simultaneously, the power demand increases faster than the power system is upgraded, creating a more stressed operation [7]. These factors make it important to utilize the power system optimally, and in a way that ensures delivered power without the risk of failures in the system. The power system is designed to be able to handle faults without significant consequences. The N-1 criterion [39] exists in the Nordic power system and states that a system should be able to withstand a fault or outage of any component.

The transmission constraints of a power system are essential for how the power system is utilized. The transmission lines can be a limiting factor of the power system, as overrated lines can cause failures or even blackouts. In order to utilize the capacity of the power system optimally, it is important to set good transmission constraints. Too conservative constraints will cause a lower capacity and price differences between price areas, and non-conservative constraints can increase the risk of failure or blackouts in the case of a disturbance. The transmission constraints in a power system are often decided by the thermal rating or the security rating of the transmission lines. The security rating refers to the rating determined by the stability limits of voltage, rotor angle, and frequency. It is expected that it is the voltage stability or the transient stability that decides the security rating in a power system. Frequency stability is mostly related to sufficient reserves in the system, making lost production or lost import the main issue.

The work of this master's thesis is a continuation of the specialization project [16] that was written during the fall of 2019.

1.2 Objective

This master's thesis aims to perform dynamic simulation on a 4-bus model and the N44 test system [22] for the purpose of deciding the transmission constraints on selected lines for optimal power flow studies. The dynamic simulations includes contingency simulations to analyze the voltage stability, and simulations of short circuits faults to analyze the rotor angle stability. The optimal power flow on the N44 test system will be simulated after a contingency and for several transmission constraints to investigating the redispatch and the change in operating costs for different transmission constraints.

1.3 Scope of work

During the specialization project, it was illustrated how the transmission constraints affect the optimal power flow, and hence how important it is to set good constraints. This thesis will continue the work of deciding the transmission constraints from the system stability.

Throughout the project, several models have been utilized. For illustrations on how the system stability is affected by the contingencies, a 4-bus model with two generators and two loads have been used. When the voltage stability was investigated, two tap-changing transformers were added between the loads and the grid to simulate dynamic loading. In addition to voltage stability, rotor angel stability was illustrated by investigating the critical clearing time at different operating states. The damping of the system was also explored by analyzing the eigenvalues of the system. The controllers were manipulated, and the power flow of the transmission lines was increased to create different cases with different damping.

Similar simulations and analyses were performed on a more advanced and realistic model of a power system to analyze how the system stability will affect the constraints in real life. The N44 model of the Nordic power system was used for this. The focus was on the power transmission on the two lines connecting Eastern Norway to Sweden as a significant amount of the exchange with Sweden flows through these lines. It was created six different cases with adjusted power flows, to analyze the effect of a contingency of one of the lines in the connection between Eastern Norway and Sweden.

By analyzing the results from the dynamic simulations, the transmission constraints for the optimal power flow were decided. The models were converted into MATPOWER casefiles, where the constraints were implemented. In Matlab®, optimal power flow simulations were performed in order to analyze the effect and cost of the transmission constraints.

1.4 Thesis outline

This thesis is organized as follows. In chapter 2, a summary of the theoretical concepts that are relevant in this thesis is given, including power system operation, line rating, power system stability, and security-constrained optimal power flow. Chapter 3 follows with an introduction of the software an the models that have been used for simulations and analysis. It also includes the methodology for the models which explains how the simulations and analyses were performed. The results from the simulations are presented and discussed in chapter 4.

2 Theory

The theoretical background in this thesis is based on the specialization project [16], where several of the concepts were thoroughly explained. This chapter includes a recap of the most important concepts that will be discussed in this thesis, as well as some new ones.

2.1 Power system operation

It is essential to produce an equal amount of energy as what is being consumed, as electricity cannot be stored in the grid. The instantaneous balance, and hence the continuous balancing, is crucial for the operational security of the power system. [43]

It is the transmission system operators (TSOs) that are responsible for controlling and operating the transmission grid, and also to ensure acceptable operations [34]. In Norway, the TSO is Statnett, and it is their responsibility to ensure balance between consumption, production, and power exchange in the Norwegian power system. In case of disturbances, it is the responsibility of Statnett to maintain balance, or in the worst case, restore balance. As the Nordic countries all share frequency and synchronism, the TSOs are cooperating to ensure balance in the Nordic power system. [43]

Statnett is also responsible for calculating the available transmission capacity in the Norwegian power system. In Norway, the main principle for determining the transmission capacity is to operate by the N-1 criterion. The N-1 criterion states that a fault on one component does not cause lost load or overloading of other components. The transmission capacities into geographical areas are hence calculated as the sum of two or more lines, with the requirement that, in the case of a contingency of the strongest component, the remaining grid can handle the loading. It is, however, not possible to maintain the N-1 criterion at all times, and Statnett has, therefore, some requirements for the operating security. These can be found in [43].

2.1.1 The Nordic power market

The Nordic power system is designed to ensure reliable power supply in every situation possible, including the power tops occurring when the demand is high,

and significant amounts of import in dry years. The capacity of the grid is also required to handle large amounts of export for times when the demand is low, and the production is high. The variations in the power flow create a need for sufficient transmission capacity, both between regions within the countries and between the countries. [13]

The power market plays an essential part in ensuring balance between production and demand. The Nordic power system is market-based. It is a natural monopoly and ensures efficient use of resources and reasonable electricity prices. Nord Pool is the power exchange for the Nordic countries. [14]

The Nordic power market is divided into a day-ahead market, Elspot, and an intraday market, Elbas. The day-ahead market is the primary market for power trading in the Nordic region, and this is where the larges volumes are traded on Nord Pool. Participants make bids and offers between 08:00 and 12:00 each day, and contracts for the delivery of physical power hour-by-hour the next day is created. The intraday marked enables trade from two hours after the day-ahead market closes and until one hour before delivery. This market makes it possible to adjust production plans closer to real-time, to ensure balance in the power system. It is, however, necessary to have reserves, and these are handles in the balancing market. [30] [47]

The Nordic power market is a shared power market for the Nordic countries, and it is divided into several price areas. These are shown in fig. 2.1. The price areas are market areas for reporting bids and offers of power on the power exchange. Hence, the reports of purchasing and selling power should be done specifically for every price area for each hour of the next day. The price is, in other words, not regulated by the government, but a result of the demand and offers of power that were reported to the power exchange in the specific market area. The differences in prices are related to the variation in available transmission capacity (ATC) between the price areas, as this congests the flow [44].

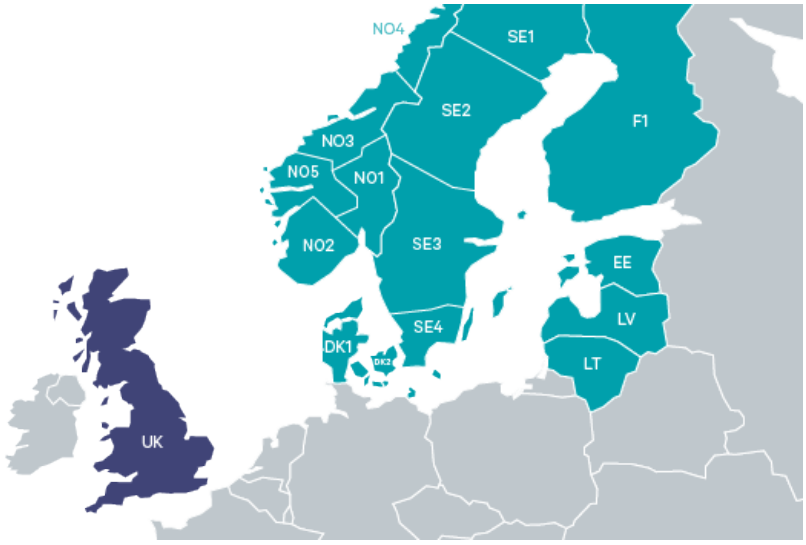

Figure 2.1: Price areas in the Nordic power system. [31]

The power market situation in each area will decide which direction the power flows between the price areas. In deficit areas, where there is a shortage of energy, the power producer will typically set a high price. The high price will lead to low power production to save the resources for emergency situations. In surplus areas, where there is plenty of energy available to cover the demand, the opposite price signal will be observed. The power producers set low prices, which leads to cheap resources that will not gain greater value in the future. The result will be high production for low prices in surplus areas, and low production for high prices in deficit areas. The power will thus flow from surplus areas to deficit areas. Also, in areas with a shortage of energy, the high prices will contribute to lower the consumption. This way, the price areas will contribute to reducing the danger of locally or regionally power deficit. [44]

2.1.2 Congestion management

The reconstruction and deregulation of the power industries around the world have caused major problems related to congestion in the transmission lines. Congestion is referred to as overloading on a transmission line caused by violated thermal rating or line capacity. It occurs when transmission networks are not able to accommodate the desired transactions due to violations of the system operating limit, or when the power flow in the transmission line exceeds the operating reliability limits. Congestion management methods can manage problems caused by congestion. There exist several methods of congestion management, such as Generators Rescheduling, load shedding, Distributed Generation, Optimal Power Flow, Flex-

ible Alternating Current Transformer System devices, Genetic Algorithms, and Particle Swarm Optimization. [49]

In [47], it is illustrated how area pricing is used in congestion management. The example starts with two areas, surplus area A and deficit area B. With sufficient capacity, power will flow from A to B without significant price differences. If the price in A is lowered or the price in B is raised, the flow will be reduced. If the transfer capacity between the two areas is reached, a price difference will occur. The transfer of power from a low price to a high price area creates a trading surplus, which is called congestion rent. The congestion rent goes to the system operator, the power exchange, or the grid company. The consequence of having limited transfer capacity is illustrated in fig. 2.2. Optimal congestion management means that the price is adjusted precisely so much that the transferred power matches the available capacity.

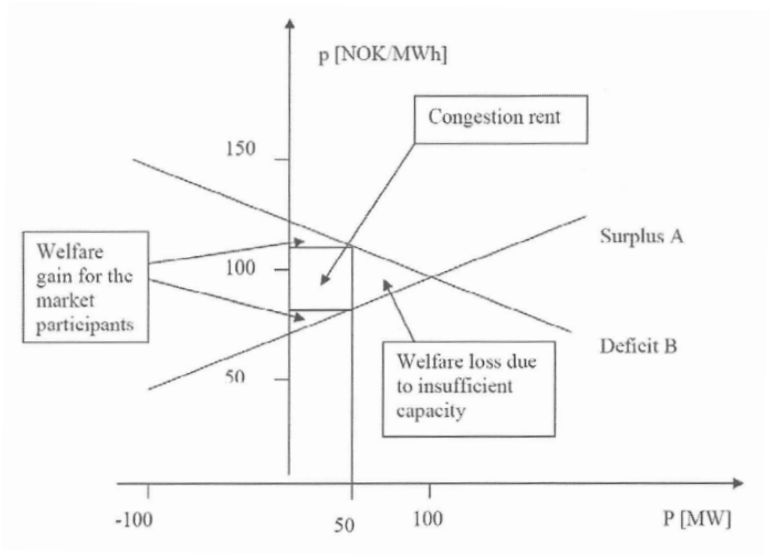

Figure 2.2: Illustration of 50 MW transfer capacity between surplus area A and deficit area B. [47]

An important congestion management method is redispatching. Redispatching is defined as rearranging the generation schedule to obtain a feasible solution that respects the transmission constraints. This method is especially useful in power systems with rapid deployment of renewable energy, as congestion become more common in such systems. Renewable energy sources can often be unpredictable, making it hard to schedule the production. Resdispatching is a great tool for the TSO to relieve the congestion that occurs on short term, in order to maintain the balance in the system. [6]

The importance of congestion management is discussed in [11]. They state that it is an essential element in the liberalization of the power industry. Like illustrated in [47], congestion can lead to price differences in the price areas of a power market. Price differences lead to financial losses, and an important issue is how costs and revenues from the congestion are shared between the market operators. Such economical issues can be solved by the use of congestion management.

2.2 Line rating

The rating of a transmission line decides the constraints related to the transmission capacity. The limiting factors can be the thermal line rating [1] and the dynamic line rating [17]. The thermal rating of a transmission line indicates the maximum power or current that can be transferred over the line without causing failure or damage. The dynamic rating of a transmission line is, however, decided by the stability of the power system. The length of a transmission line determines its limiting factor. This is illustrated in fig. 2.3. It can be seen that the thermal line rating will limit transmission lines with lengths below L, and the dynamic security rating will limit transmission lines with lengths above L.

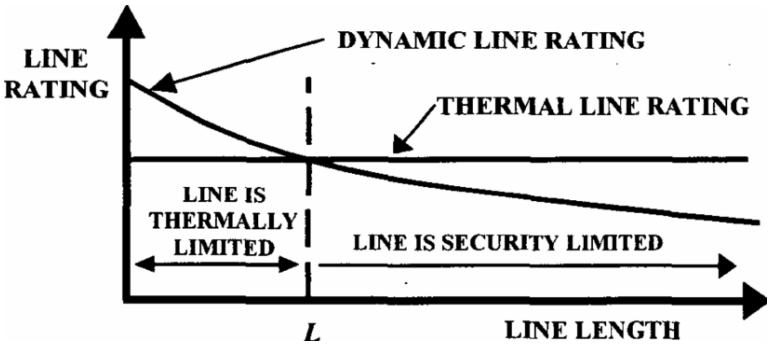

Figure 2.3: Dynamic and thermal ratings of an overhead transmission line. [4]

The consequences of loading a transmission line above the line rating can be fatal. If the thermal rating is exceeded, the temperature of the line can become too high, and this excessive temperature can cause sagging in the transmission line and result in the line contacting the surroundings [1][4]. Similarly, exceeding the dynamic security ratings can cause stability issues resulting in, for instance, a voltage collapse.

It is common to divide thermal line rating into static and dynamic thermal rating. In [1], it is explained that the static thermal line rating is calculated from seasonal temperatures, maximum solar heating, and low wind speed. This rating is held

constant, but it is possible to calculate the static thermal line rating for several cases, as it will vary depending on the season and also on operations. Douglass et al. [1] explain that the dynamic thermal line rating, however, varies from hour to hour. It is calculated similarly to the static thermal lime rating, but when it is recalculated every hour, it is possible to include the current weather conditions in the calculations. Dynamic thermal ratings will thus be more accurate than static thermal ratings and make it possible to utilize the power system more efficiently. In addition to this, there may exist thermal line ratings for normal conditions, for short-term emergency operation post contingencies, and long-term emergency operations post contingencies.

In [17], it is explained how the dynamic security rating of a transmission line relates to the phase angle difference across the line and how it is a function of line admittance. Longer transmission lines have larger angular phase differences for a line loading, which is illustrated in fig. 2.3. Transmission lines are also dependent on the voltage at each end of the line, creating a stability limit. The system becomes unstable when the point of maximum loadability is reached. The point of maximum loadability indicates how much power that can be transferred over the transmission line. Most extra high voltage lines are loaded to a limit determined by stability consideration, which is lower than the thermal limit of the extra high voltage lines [4].

2.3 Power system stability

This section includes a description of power system stability and some concepts that will be discussed and analyzed throughout this thesis. Power system stability can be defined as the ability of a power system to regain a state of operation after being subjected to a disturbance, such that the system remains intact [25].

The classification of power system stability is shown in fig. 2.4. It is divided into three categories; rotor angle stability, voltage stability, and frequency stability, with several subcategories.

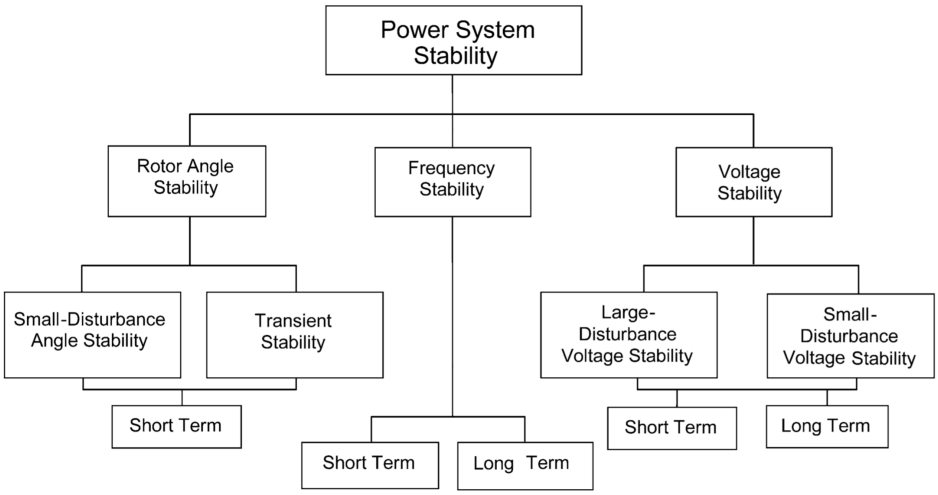

Figure 2.4: Classification of power system stability. [25]

In this thesis, rotor angle stability and voltage stability will be analyzed for a 4-bus model and for a the N44 test system to investigate the stability limits. Frequency stability will not be considered to the same extent because stability issues related to frequency are usually associated with adequate reserves.

2.3.1 Voltage stability

Voltage stability is of significant interest in power system operation and planning as the electrical power systems are becoming more and more complex, and transmission lines are operating closer to their limits [8].

Kundur et al. [25] define voltage stability as the ability of a power system to maintain the steady-state voltage at all buses in the system after being subjected to a disturbance from a given initial operating condition. Maintaining equilibrium between demand and production in the power system is essential for voltage stability. Instability in voltage occurs as a rise or fall in voltage on a bus. It can cause loss of load in an area, tripping of transmission lines, and other elements by their protective system leading to cascading outages. Such outages may result in a loss of synchronism.

Voltage stability and rotor angle stability are closely related, and a voltage drop can be associated with instability in the rotor angle. As an example, consider two groups of machines. A loss in synchronism causes the rotor angle between the two machines to approach 180°. When this happens, intermediate points in the network close to the electrical center experiences a rapid drop in voltage. For the

case when the system is not so separated, repeated "pole-slips" will occur between the two groups of machines, causing oscillations in voltages near the electrical center. However, voltage instability can also be caused by a change in load and can occur independently of the rotor angle instability. [25]

The term *voltage collapse* is frequently used about the sequence of events causing voltage instability that leads to a blackout or abnormally low voltage in a significant part of the system. The most common form of voltage instability is the progressive drop in voltage, which can be caused by the loads. After the occurrence of a disturbance, the loads are restored by the action of, for instance, motor slip adjustment, voltage regulators, and tap-changing transformer. The restoring increases the reactive power consumption, which causes an increase in the stress on the high voltage network. Hence, the voltage is further reduced and causes problems regarding voltage stability. [25]

2.3.1.1 Load modeling

It is generally agreed upon that the voltage stability analysis of a system is significantly affected by the load modelling [8][32][50]. Consequently, it is essential to represent the loads properly when performing voltage stability assessments. As it is not practical to model every load and its control device in detail, it is useful to use a load model that describes the generic behavior of the load. Chakrabarti [8] states that load flow programs usually assumes that the load active and reactive power remain constant of load voltage. The constant load will give a misleading and pessimistic result because the available power margin is minimum. Loads can be modeled statically by the exponential load model given in eq. (2.1) where P and Q are the active and reactive powers consumed by the load at voltage V, and P_0 and Q_0 are the active and reactive power consumed by the load at V_0. α and β are the load exponents.

$$P = P_0(\frac{V}{V_0})^{\alpha} \tag{2.1a}$$

$$Q = Q_0(\frac{V}{V_0})^{\beta} \tag{2.1b}$$

The values of α and β can be changed in order to change the load model between constant power loads, constant current loads, and constant impedance loads. It is not very reasonable to model the loads by a single term because power system loads are combinations of components having different power to voltage sensitivities, and this can be solved by using a polynomial load model. The load model used in dynamic studies in PSS®E is the ZIP Model. The ZIP Model [3] represents the relationship between the voltage magnitude and power in a polynomial equation that combines constant impedance (Z), current (I), and power (P) components.

A load model which is dependant on voltage will give a more robust system in the case of voltage stability, as the load will decrease for higher voltages closer to the stability limit. However, in cases where the system is in fault, dynamic load models should be used [32]. Such a dynamic load model can be the exponential recovery load model presented in [3].

In PSS®E, it was beneficial to model recovering loads by implementing tap-changing transformers between the grid and the loads. On-load tap-changing transformers are devices that can change taps while they are energized and carry load [19]. They are widely used in smart distribution grids because of their ability to regulate and maintain voltage [46]. The voltage regulation is performed by altering the winding ratio. In the 4-bus model with dynamic loads used in this thesis, the tap-changing transformers were implemented to alter the winding ratio when the voltage on the load side of the transformers exceeded the voltage limits.

2.3.1.2 PV curves

The power-voltage (PV) curve [24] is an important tool in analyzing the voltage stability of a system. It indicates the maximum power the system can carry before the voltage collapses, and the system becomes unstable. The maximum power point is located at the tip of the curve. In fig. 2.5, the voltage is plotted as a function of the real load creating a PV curve. As the tip of the curve indicates the voltage stability limit. The system is stable in the upper part of the PV curve, and the tip of the curve shows the voltage stability limit. The PV curve is also used to investigate at which load the system exceeds the acceptable voltage limits.

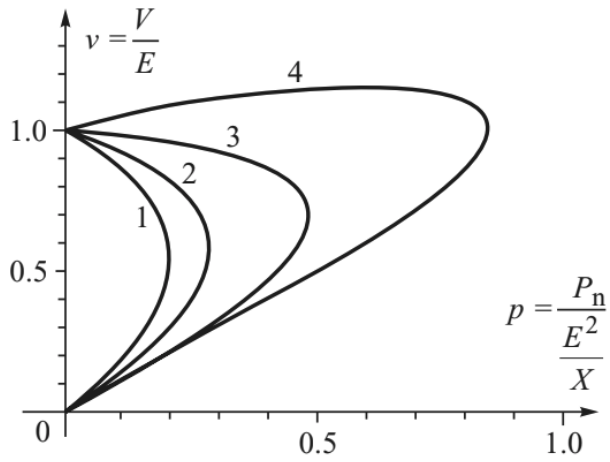

Figure 2.5: PV curves with different power angles, ϕ, (1) $\phi = 45°$ lag, (2) $\phi = 30°$ lag, (3) $\phi = 0$, (4) $\phi = 20°$ lead. [26]

Figure 2.5 shows different PV curves for different power angles, and it illustrates how the voltage is dependant on real load. The voltage level decreases as the real load increses. It can also be observed that the power angle, and hence the power factor, affects the critical point of the system and that an increased, leading power angle makes it possible to supply more load to the system. For an increased, lagging power angle, the opposite is observed, as the amount of power that is possible to supply to the system is decreased. [24][26]

2.3.2 Rotor angle stability

Rotor angle stability is related to the synchronism of the synchronous machines in a power system. It refers to their ability to remain in synchronism after being subjected to a disturbance. When the equilibrium between electromechanical torque and mechanical torque is lost, instability, or loss of synchronism, occurs. Rotor angles stability is divided into two subcategories, small-disturbance angle stability and transient stability [25]. Small-disturbance angle stability refers to the ability of the system to remain stable, in synchronism, after small disturbances. Transient stability refers to the ability of the system to remain in synchronism after being subjected to a large disturbance. A short circuit on a transmission line is an example of such a disturbance [26].

2.3.2.1 Equal Area Criterion

The equal area criterion is a technique for analyzing the transient stability of a power system. The procedure is illustrated for a three-phase fault in figure fig. 2.6.

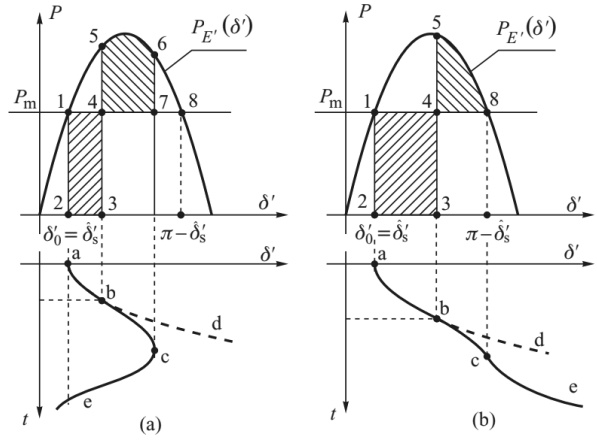

Figure 2.6: The equal area criterion illustrated for (1) short clearing time, stable case, and (b) long clearing time, unstable case. [26]

For this simple illustration, it is assumed that the fault is cleared without any changes in the equivalent network impedance. Also, the mechanical power from the turbine is assumed to be constant, and the damping is neglected [26]. Figure 2.6 shows the power-angle curve of a generator when it is subjected to a three-phase fault. The generator gets blocked from the rest of the system when the fault occurs, which causes the electrical power to drop to zero, point 2 in fig. 2.6(a). The electrical power remains at zero until point 3, where the fault is cleared. At this stage, the rotor has obtained kinetic energy proportional to the shaded area 1-2-3-4. When the fault is cleared, the electrical energy will follow the power-angle characteristic and jump directly to point 5. The rotor will now experience a deceleration torque. However, the angle will keep increasing until the work done during deceleration is equal to the kinetic energy obtained during acceleration, i.e., until the area 4-5-6-7 equals the area 1-2-3-4. When the areas are equal at point 6, the rotor reaches synchronous speed. For a system without damping, the rotor will keep swinging back and forth around point 1. This is called synchronous swings, meaning that the generator does not lose synchronism, and the system is stable.

Figure 2.6(b) illustrates a situation where the clearing time is longer. In this case, the kinetic energy obtained in the acceleration stage is too high for it all to be absorbed by the work performed in the deceleration stage. This results in the rotor making an asynchronous rotation and losing synchronism with the system. When the synchronism is lost, the system becomes unstable in the sense of transient stability.

In other words, the available deceleration area has to be larger than the acceleration area, area 4-5-8 > area 1-2-3-4, for the system to be transient stable. The transient stability limit can be defined as in eq. (2.2). It can also be transferred to the critical clearing time, t_{cr}, which is the longest clearing time for which the generator will remain in synchronism.

$$K_{area} = \frac{\text{area } 6-7-8}{\text{area } 4-5-8} \tag{2.2}$$

Another measure for the transient stability margin is given in eq. (2.3), where t_f is the actual clearing time. [26]

$$K_{time} = \frac{t_{cr} - t_f}{t_{cr}} \tag{2.3}$$

This example of how the equal area criterion can be used to analyze the stability of a system is quite simple. Most real-life situations are more complex than this. A fault will not be cleared by itself, and the faulted element, e.g., the line, needs to be disconnected after the fault. The equal area criterion can nevertheless be used to analyze a real-life three-phase fault, as the process is similar with some

adjustments.

The mechanical power input P_m will also affect the transient stability. In the illustrations in fig. 2.6, P_m is constant. By increasing or decreasing P_m, it can be observed that the acceleration area, area 1-2-3-4, and the deceleration area, area 4-5-8, will change. A lower P_m will give a larger deceleration area, which indicates that the critical clearing time of the system is increased. For the opposite case, with a higher P_m, the deceleration area, and hence the critical clearing time, is decreased.

2.3.2.2 Eigenvalue analysis

Eigenvalue analysis is a powerful tool for studying the small-signal stability of a power system [41]. It is used for simplifying a large dynamic system by representing the system response to a disturbance as a linear combination of uncoupled aperiodic and oscillatory responses. The mathematical background of the linear representation and eigenvalues are described closer in [26].

Eigenvalues can be both real and complex numbers and are usually presented in the complex plane. A stable system has eigenvalues in the left half of the complex plane, hence with negative real parts. Further on, the eigenvalues give important information on the oscillations and damping of the time responses of the system. In [5], it is explained that a system with eigenvectors with an increased imaginary part will experience higher frequency in oscillations, and a system with eigenvectors with increased real parts will experience more damping.

The small-signal stability performance of large power systems has become a more important stability issue due to the rapidly changing power system. The growth in installed capacity and system loading may cause operators to operate closer to the stability limits. In large interconnected power systems, inter-area oscillating has hence become common and can cause stability issues. In such large systems, inter-area oscillations are a common problem, and in cases where more power is transferred over longer distances, it can be the primary stability limit as the electromechanical oscillations can become less damped [45]. Eigenvalue analysis is a useful tool to analyze these oscillations because the dynamic behavior of a linearized power system model can be investigated. It is required that all modes of the linearized system are stable, and it is desired that they are adequately damped. An eigenvalue calculation gives the damping, the frequency, and the damping ratio of the modes. There is no known minimum damping requirement, but a damping ratio of more than -3% has to be taking with caution. Also, the damping is considered adequately, if the damping ratio of the electromechanical modes are max. -5%. [36]

The eigenvector of a system can also be analyzed using modal analysis, and they give important information about the oscillatory modes. The right eigenvector

gives information about the observability, while the left eigenvector gives information about the controllability. The combination of the two indicates a good damping location. It is very important to ensure adequate damping of inter-area oscillation. The oscillations can be damped by injecting extra energy into the system to decelerate it. The effect is vice-versa when the energy is consumed by the system. The damping energy must have the correct phase shift relative to the accelerated/decelerated system because an incorrect phase angle can result in excited power oscillations. [26] [36]

2.4 Security Constrained Optimal Power Flow

Power flow studies are used for planning, operation, economic scheduling, and exchange of power between utility [33]. For that reason, it is a very important part of the power system analysis. For a system operating under normal conditions, there exist multiple solutions for scheduling generation, as the generation capacity is higher than the power demand. The optimal power flow (OPF) is a useful tool for deciding how to schedule the generation of a system.

The OPF problem is an optimization problem with the objective of minimizing the operating cost when finding the real and reactive power scheduled for each power plant in an interconnected system. The objective function in the problem formulation is a cost function presenting economic cost, system security, and/or other objectives. To find the optimal operating point, the cost function is minimized. The constraints in the OPF problem ensures that the optimal operating point is found within acceptable system performance. [33]

The Security Constrained Optimal Power Flow (SCOPF) [7][10] is an extension of the OPF problem, which includes additional constraints related to the operation of the system under a set of contingencies. Such constraints will assure satisfying operating conditions in the post-contingency steady-state, although the operating costs are optimized in the pre-contingency state.

The SCOPF problem is evolved because there are several challenges related to the OPF problem. The power system is developing quite fast, and today it is operating in more "stressed" conditions that what was expected in the planning stage. The load has increased without sufficient upgrade in generation and transmission systems, as well as the electricity markets has led to trading large amounts of electrical energy over long distances. In addition to this, the growth in renewable energy sources causes more uncertain operating conditions. The day-ahead operational planning by the TSOs has thus become an exercise in managing uncertainty in which the SCOPF plays an important role. [7]

There are several issues related to the SCOPF that makes it much more challenging than the OPF problem. These are, for instance, the significantly larger problem

size, the need to handle more discrete variables describing control actions, and the variety of corrective control strategies in the post-contingency states. [7]

2.4.1 Formulation of the SCOPF problem

The conventional SCOPF problem can be formulated as follows [7]:

$$\min_{\boldsymbol{x}_0,\ldots,\boldsymbol{x}_c,\boldsymbol{u}_0,\ldots,\boldsymbol{u}_c} f_0(\boldsymbol{x}_0,\boldsymbol{u}_0) \tag{2.4a}$$

$$\text{subject to:} \quad g_0(\boldsymbol{x}_0,\boldsymbol{u}_0) = \boldsymbol{0} \tag{2.4b}$$

$$h_0(\boldsymbol{x}_0,\boldsymbol{u}_0) \leq \boldsymbol{L}_l \tag{2.4c}$$

$$g_k^s(\boldsymbol{x}_k^s,\boldsymbol{u}_0) = \boldsymbol{0} \qquad k = 1,\ldots,c \tag{2.4d}$$

$$h_k^s(\boldsymbol{x}_k^s,\boldsymbol{u}_0) \leq \boldsymbol{L}_s \qquad k = 1,\ldots,c \tag{2.4e}$$

$$g_k(\boldsymbol{x}_k,\boldsymbol{u}_0) = \boldsymbol{0} \qquad k = 1,\ldots,c \tag{2.4f}$$

$$h_k(\boldsymbol{x}_k,\boldsymbol{u}_0) \leq \boldsymbol{L}_m \qquad k = 1,\ldots,c \tag{2.4g}$$

$$\boldsymbol{u}_k - \boldsymbol{u}_0 \leq \overline{\Delta \boldsymbol{u}}_k \qquad k = 1,\ldots,c \tag{2.4h}$$

The objective function, f_0, corresponds to the pre-contingency configurations. The variable k is indicating which contingency the system is subjected to, where 0 indicates pre-contingency, and c is the total number of contingencies. $\boldsymbol{x}_k$ is the vector of the state variables, $\boldsymbol{x}_k^s$ is a vector of the state variables in the short term time frame, and $\boldsymbol{u}_k$ is the vector of control variables. $\overline{\Delta \boldsymbol{u}}_k$ is the vector of the maximum allowed adjustments of the control variables between the base case and the k-th post-contingency state. The limits are denoted $\boldsymbol{L}$, where the subtext l is for long-term, or normal, operation, s is for short-term operation, and m is for medium-term operation.

This problem formulation contains two types of constraints; the equality constraints, (2.4b, 2.4d, 2.4f), and the inequality constraints, (2.4c, 2.4e, 2.4g). The equality constraints represent the AC load flow equations and ensure balance in production and load. The inequality constraints include the limits of the system, i.e., the physical limits of the equipment and the operational limits on the branches. The limits are defined by the TSOs, and they have to satisfy $\boldsymbol{L}_l \leq \boldsymbol{L}_m \leq \boldsymbol{L}_s$.

The subscript 0 indicates the pre-contigency state, as mentioned before, which means that the constraints (2.4b, 2.4c) enforce feasibility on the pre-contingency state. The constraints (2.4d, 2.4e) and (2.4f, 2.4g) enforce feasibility post-contingency, and the superscript s in (2.4d, 2.4e) denotes short term, and the other constraints refer to medium term.

The system dynamics are not usually modeled in the conventional SCOPF problem formulation. It is, nevertheless, an assumption inthe conventional SCOPF that the system does not lose stability after the occurrence of a contingency. The SCOPF

is, for this reason, often formulated in a conservative way by imposing strong constraints, which leads to sub-optimal operations. Some simplified representations of dynamics in SCOPF are reviewed in [7], where it is described how both transient and voltage stability can be handled in the SCOPF.

2.4.1.1 Preventive SCOPF

There exists a particular formulation of the SCOPF problem that does not consider the possibility of corrective actions in states after the contingency, other than those that take place automatically [7]. This formulation is called the "preventative" SCOPF (PSCOPF), and it assumes that steady-state conditions can be met after the contingency without redispatching. In real life, this is the dominating method of SCOPF because power flows and voltages need to remain within operating limits, as the likelihood of blackout increases even for short-term transmission line overloads [10].

3 Methodology

In the following chapter, the software, model description, and methodology is covered. The models do not have the same methodology, and hence the methodology is divided into two section; one for each model.

3.1 Software

3.1.1 PSS®E

PSS®E is a high-performance transmission planning and analysis software developed by Siemens. It is widely used across the world and is one of the leading power transmission simulation and analysis tools. PSS®E has several analysis functions, like power flow, dynamics, and stability analysis [38]. In this thesis, it is mainly used from a Python interface by using the Psspy API [35] to perform contingency analysis and investigating voltage and transient stability.

3.1.2 Psspy Python framework

Psspy is a Python package that allows for Python to interface with PSS®E. This way, the initialization of models, changing of parameters, and running of simulations can be done automatically by running a Python code.

3.1.3 Pycont

The simulations related to the dynamic analysis in this thesis were performed in the tool Pycont, which is owned by SINTEF Energy Research. This is a contingency simulation tool that allows for both static and dynamic contingency simulation. It is written in python 2.7, and uses the Psspy API [35] to perform simulation in PSS®E.

Pycont includes several classes, where four were used for the simulations in this thesis. PycontConf is the class that reads all configurations that are given for the relevant case. This includes e.g., the grid files, the list contingencies, and the generator and load data for the different operating states. The class PsseGrid

is used for interfacing with PSS®E and includes all functionality that is related to simulations in PSS®E. Pycont is able to run simulations for multiple operating states, and the class OperatingStates is responsible for setting the correct operating. Finally, the contingencies are run by the class ContAnalysis.

The steps for running a dynamic simulation in Pycont is thus to

1. define all configurations in the additional files,
2. configure this in the class PycontConf,
3. establish a grid in the class PsseGrid based on the configurations,
4. define the contingencies in ContAnalysis, and
5. run the contingency analysis.

3.1.4 DIgSILENT PowerFactory

PowerFactory is a leading power system analysis software application for use in analyzing generation, transmission, distribution, and industrial systems [9]. In this thesis, the eigenvalue analysis was performed in PowerFactory.

3.1.5 MATPOWER in MATLAB®

MATPOWER is a tool for solving steady-state power system simulations and optimization problems [27]. The optimal power flow simulations were performed using the function `runopf()` on the relevant case file representing the model.

3.2 Model description

3.2.1 4-bus model

The 4-bus model is a network model consisting of two generator buses and two load buses. A figure representing the model is given in fig. 3.1. The model is similar to the model used in the specialization project [16], but with a few adjustments. The machine base value of the generator was adjusted to better match the dynamic model. In addition, the base value of the voltage was increased to 420 kV, and the reactance was decreased to 0.05 p.u. to obtain an acceptable voltage. The network data and dynamic data of the model is given in appendix A and appendix B, respectively.

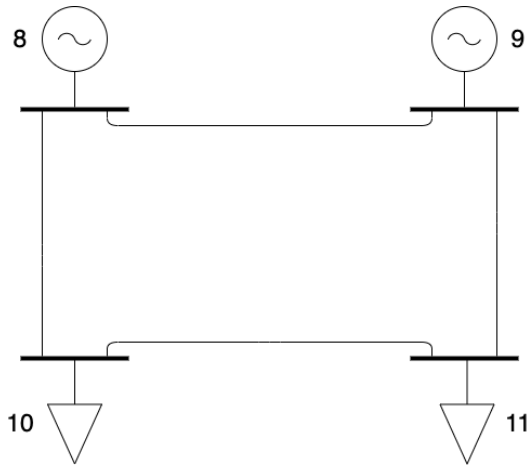

Figure 3.1: 4-bus model.

3.2.2 4-bus model with dynamic loads

The 4-bus model with dynamic loads is an extension of the 4-bus model described above. The stiff loads are substituted by dynamic loads. To obtain dynamic loads in PSS®E, tap-changing transformers were added to both loads. This is shown in fig. 3.2.

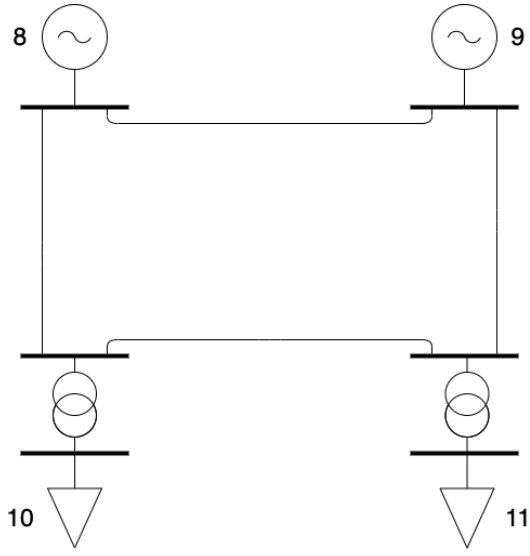

Figure 3.2: 4-bus model with dynamic loads.

The transformers were added to the model with voltage as the control mode. The values used in the model are given in table A.6 in appendix A. This table includes the most important values of the transformers, hence the ones that were changed from the default values. Among these values are the impedances, the maximum and minimum value of the ratio of the transformer, and the control parameter. The remaining values in the PSS®E model of the transformers were set to the default values.

In the dynamic model, the OLTC1T model was utilized. This is a 2-winding transformer online tap changer model [37]. The tuning that were used in the simulations are given in table B.4 in appendix B.

3.2.3 The Nordic 44 test system

The 4-bus model is useful for illustrating concepts but does not give a particularly realistic image of how a real power system would respond. Hence, the Nordic 44 (N44) network model, which is a more extensive and realistic test system, is introduced. The N44 network model [22] is a simplified representation of the Nordic grid, and it is designed for analysis of dynamic phenomena. The model is obtained from [20]. In fig. 3.3, a graphical illustration of the model is given.

To limit the scope, the focus will be on the transmission between eastern Norway and Sweden. This is a line with a capacity of 2000 MW, which handles a great amount of the export from Norway to Sweden [18]. This makes it interesting to investigate how the stability of the system is affected by a contingency on one of the lines in this transmission for different operating states. In the N44 network model, the specific lines refer to the lines connecting bus 5101 and bus 3359.

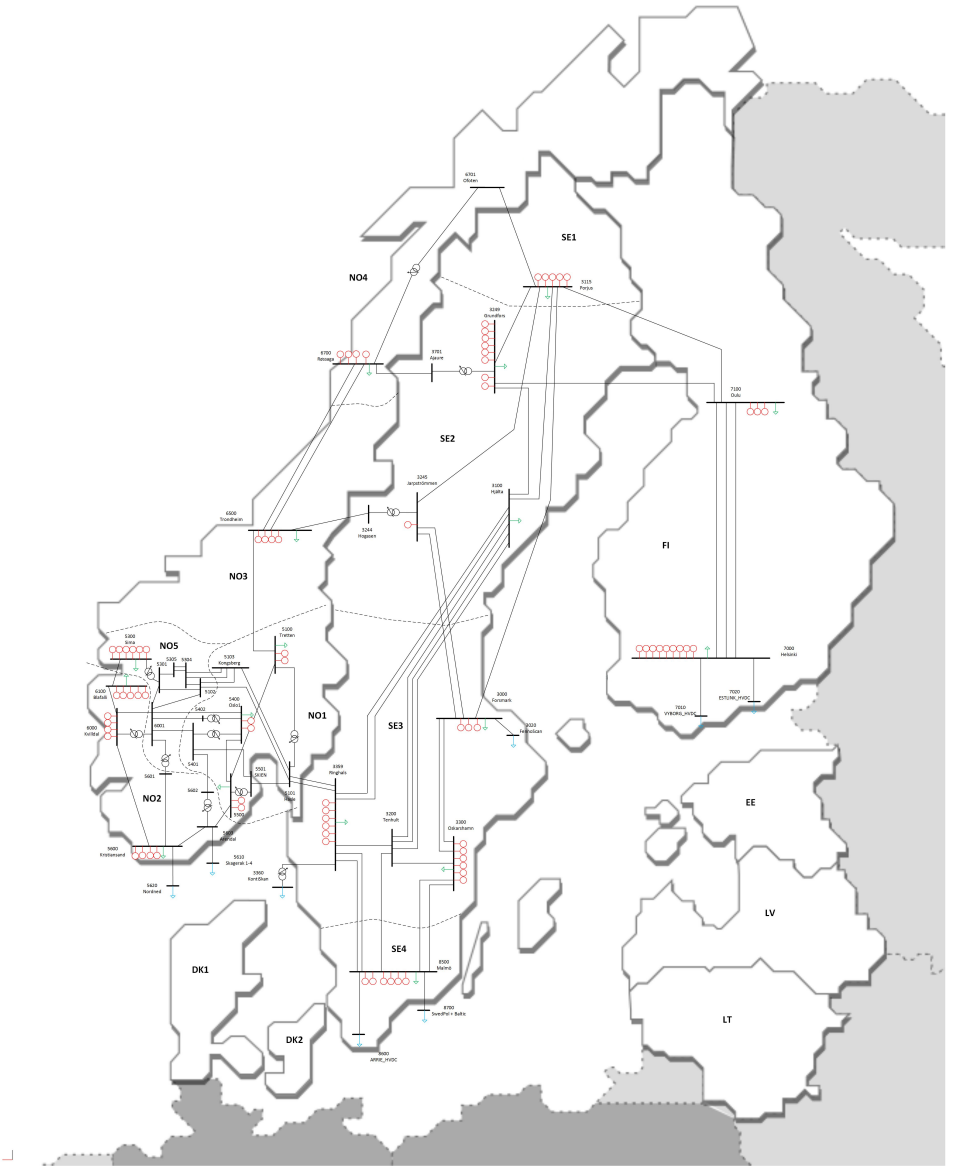

Figure 3.3: The Nordic 44 aggregated network model. [42]

3.3 4-bus model methodology

3.3.1 Contingency simulations

The dynamic contingency simulation was performed to investigate the power flow, stability issues, and damping of the system. The system was subjected to a series of contingencies given in table 3.1.

Table 3.1: The contingencies the 4-bus model was subjected to.

Contingency no.	Bus from	Bus to
1	8	9
2	8	10
3	9	11
4	10	11

The simulations were performed in the simulation tool, Pycont, in the same way as in the specialization project [16]. When the stability of the system was analyzed, it was important to simulate several operating states by varying the generation and the load on the buses. To vary the operating state systematically, a few assumptions were made. It was assumed that the total load was divided equally between load 10 and 11. Also, one of the generation buses, e.g., bus 9, was kept constant while the load was increased from 1000 MW to 2400 MW in steps of 200 MW. The generation on the other generator was calculated from eq. (3.1) when the losses were neglected. This was continued for several values of the constant production at one of the buses, from 500 MW to 1200 MW in steps of 100 MW.

$$P_{G8} = P_{load,tot} - P_{G9} \tag{3.1}$$

The output of the simulations was different plots that show the development of the chosen time variable as a function of time. As an example, the plots included the voltage at the load buses or the power flows on the transmission lines. These plots were used in analyzing how the stability of the system was affected by the disturbance for the different operating states described above.

3.3.2 Rotor angle stability

The rotor angle stability of a system is dependant on the clearing time after a fault. It was therefore of interest to analyze the clearing time of the system to find the critical clearing time. For this analysis, it was chosen to focus on the fault on the line connecting bus 8 and 10, corresponding to contingency 2. To investigate how

the critical clearing time, t_cr, after this fault was affected by different parameters, the electrical power, and relative rotor angle was analyzed. The critical clearing time was found when the oscillations in the electrical power was not damped, and when the rotor angle no longer stabilized after a fault but continued to increase.

The critical clearing time was found for several operating states to analyze how it was affected by the total load of the system and how the generation was distributed between the two generators. During all simulations, the system was subjected to a branch fault followed by a contingency of the line connecting bus 8 and 10. The clearing time after the disturbance was varied until the critical clearing time was found for every operating state. The total load and generation were varied as described in section 3.3.1, and the generation on bus 8 was kept constant.

3.3.3 Voltage stability

To analyze the voltage stability of the power system, it was necessary to define acceptable limits for the voltage value. The most known and used limit for voltage is to allow a variation from the nominal value of $\pm 10\%$ [2]. This means that a voltage that stabilized outside this limit after a disturbance is not acceptable, regardless of the oscillations of the response. The voltage can thus be stable in the sense of voltage stability, but yet not acceptable. These limits are set in order to maintain a satisfactory quality of voltage. Voltage responses that do not stabilize due to lack of damping or voltage collapse is obviously not acceptable either.

To investigate how the voltage stability was affected by the total load and the generation, the value of where the voltage stabilized was noted for different operating states. The operating states were varied as described in section 3.3.1 and with a constant generation on bus 8. This was performed on the 4-bus model and on the 4-bus model with dynamic loads to illustrate how the dynamic loads affect the voltage stability.

3.3.4 Eigenvalue analysis

The eigenvalue analysis of the system was performed in DIgSILENT PowerFactory. To investigate the stability of the system, it was of interest to analyze the eigenvalues after a disturbance. Hence a line was disconnected, and the load flow was calculated prior to the eigenvalue analysis. It was chosen to focus on the disconnection on the line 8-10 with a total load of 1000 MW and production of 500 MW at both generators.

The oscillations of a system are dependant of the controllers. To investigate how the automatic voltage regulator (AVR) and turbine governor affected the eigenvalues, and hence the stability of the system, the eigenvalue analysis were simulated for

different values of the parameters of the controllers. The values of the base case are given in appendix B.1. In the AVR, the filter delay time, Tb, and the filter derivative time constant, Ta, were decreased. In the governor, the temporary droop, r, and the governor time constant, Tr, were increased.

It was also interesting to simulate a case with increased power flow, to investigate how the flow affects the damping of the system. To do this, the total load was increased to 1600 MW, and the production at generator 8 was increased to 1100 MW.

In PowerFactory, the eigenvalue analysis was performed using the built-in QR/QZ-Method. Afterward, the eigenvalues were plotted in the complex plane and analyzed. When the eigenvectors were analyzed, the dynamic models of the AVR and turbine governor where changed in the PSS®E model in order to perform simulations in Pycont to illustrate how the time responses of the system were affected by the eigenvalues.

3.3.5 Optimal power flow

The optimal power flow simulations in this thesis were solved using MATPOWER in Matlab®. A case file was created for the 4-bus model, and the optimal power flow was solved by running the embedded function `runopf()` on this file. The input of the function is information about the buses, generators, branches and generator costs of the system and returns the production, line flows, and objective cost function value of the optimum [29].

The MATLAB® casefile created for the case contains information about the bus data, generator data, branch data, and generation cost data. The bus data matrix gives information on what bus type the different buses are, and how much load they draw. The generator data matrix provides information on the generation limits, both active and reactive, and the planned generation is also stated. The resistance and reactance of the branches are given in the branch data matrix, as well as the line ratings. There are three different line rating, where A represents the long term rating, B is the short term rating, and C is the emergency ratings. The values of the matrices are given in appendix A.

The objective function in the optimal power flow is the generator cost functions. It is a polynomial that is a function of the generation of the two generators. It is given in eq. (3.2).

$$f(P_8, P_9) = c_8 P_8^2 + c_9 P_9^2 \tag{3.2}$$

where $c_8 = 0.05$ \$/$(MW)^2h$ and $c_9 = 0.02$ \$/$(MW)^2h$.

The transmission constraints decided from the dynamic simulations were implemented in the casefile before simulating the optimal power flow. The optimal power flow was also simulated without constraints to compare the effect and cost of the transmission constraints.

3.4 Nordic 44 methodology

3.4.1 Stability analysis

The dynamic simulations and analysis performed on the Nordic 44 model were less extensive than the ones performed on the 4-bus model. For this reason, it was not necessary to rewrite Pycont to work with the new model, and it was decided to create a new script in Python using the Psspy API. The new code was based on the examples in [21], and it is given in appendix C.

The contingency simulations and analysis that were performed on the Nordic 44 model did only include one contingency, on the second line connecting bus 5101 and bus 3359. This is one of the lines that connect Eastern Norway to Sweden. To analyze the stability of the system for different operating states, the production and load in different areas of the system were varied. The six cases, in addition to the base case, that were chosen are presented below. The percentage of the increase/decrease in load and production were calculated from the values given in the base case.

Case 0 This is the base case, and the following cases are based on this.

Case 1 In this case, the production in Western Norway, bus 5300 and bus 6100, was increased by 10%, and the load in Sweden, bus 3359, was increased by 15%.

Case 2 In this case, the load in Oslo, both bus 5400 and 5500, was reduced to 1) 65% and 2) 59%, and the production in Sweden, bus 3115, was decreased to 1) 40% and 2) 30%.

Case 3 In this case, the production in Western Norway, bus 5300 and 6100, was increased by 10%, and the production in Finland, bus 7100, was decreased to 85%.

Case 4 In this case, the production in Finland, bus 7100, was increased by 25%, and the load in Oslo, bus 5400 and 5500, was increased by 10%.

Case 5 In this case, the production in Finland, bus 7100, was disconnected, and the load in Oslo, bus 5400 and 5500, was decreased to 65%.

Case 6 In this case, the production in Finland, bus 7100, was increased by 25%, and the load in Sweden, bus 3359, was increased by 10%.

The stability analysis for each case was performed very similarly to the stability analysis on the 4-bus model. The code was enhanced to make it possible to perform voltage stability analysis, frequency stability analysis, and rotor angle stability analysis. For the voltage stability analysis and the frequency stability analysis, the voltage and frequency at the load buses were plotted and analyzed after the contingency, respectively. The stability limits were defined in the code, and when the simulations were performed, it was checked if the voltage or frequency stabilized within the acceptable limits. To analyze the rotor angle stability, and hence the critical clearing time for each case, a fault followed by a clearing and contingency were simulated. The critical clearing time was found the same way as for the 4-bus model.

3.4.2 Optimal power flow analysis

The MATPOWER casefile for the N44 model was created by running the function `psse2mpc()`. The function takes in a PSS®E RAW file and converts it to a MATPOWER case struct [28]. The generator cost data was added to be able to perform OPF simulations. The model data for this model is given in appendix D. To create a case where the power flow on the line connecting Eastern Norway and Sweden where too high, the generators in Sweden were given a higher price than in Norway. The objective function is given in eq. (3.3).

$$f(P_{NO}, P_{SE}, P_{FI}) = c_{NO}P_{NO}^2 + c_{SE}P_{SE}^2 + c_{FI}P_{FI}^2 \tag{3.3}$$

where P_{NO}, P_{SE} and P_{FI} are the production of real power in Norway, Sweden and Finland, respectively, and c_{NO}, c_{SE} and c_{FI} are the price constant for the production in the respective countries. The price constants were set to $c_{NO} = c_{FI} = 0.01$ \$/$(MW)^2h$ and $c_{SE} = 0.03$ \$/$(MW)^2h$.

The OPF was simulated after a contingency of one of the lines connecting Eastern Norway and Sweden. Initially, the optimal solution was calculated without transmission constraints, and the objective function value and production on every machine where noted. Secondly, a case where only a few generators were available for redispatching was created. The generation at the unavailable generators were locked to the original production by setting the generation limit close to the original production. The machines that were decided to be available for redispatching was located in Western Norway, Southern Norway, Eastern Norway, Northern Sweden, Eastern Sweden and Northern Finland. Finally, the transmission constraint on the remaining line in the connection between Eastern Norway and Sweden were implemented. The OPF were then simulated for different values of the transmission constraint between 3200 MW and 1000 MW. For each case, the objective value function were noted to analyze the cost of the constraint, and the generation at the buses were noted to investigate which machines that were used for redispatching.

4 Results and discussion

4.1 4-bus model

When the dynamic simulations were performed in Pycont, it was observed that the contingencies between the generators and between the loads, contingency 1 and 4, did not cause particularly difficulties regarding the stability of the system. It was also found that the contingencies of the lines connecting a generator and a load caused similar stability issues. Therefore, only the results of contingency 2 is presented in this chapter.

4.1.1 Power flow

Figure 4.1 and 4.2 show the power flows on all four lines of the model for two different operating states before, during, and after a contingency of the line 8-10. The generation at bus 9 was set to 500 MW for both operating states, and the total demand was set to 1000 MW and 1600 MW, respectively.

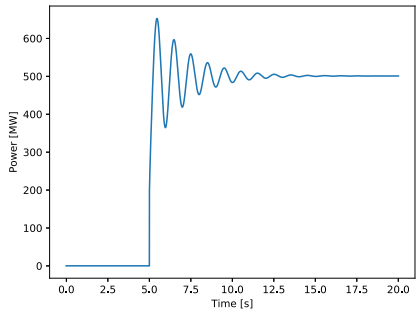

(a) Line 8-9.

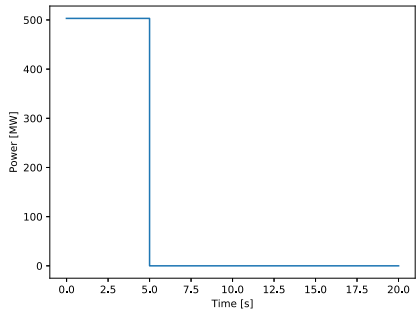

(b) Line 8-10.

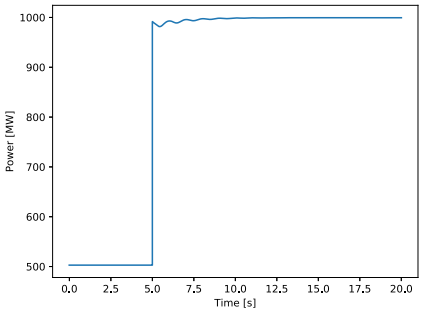

(c) Line 9-11.

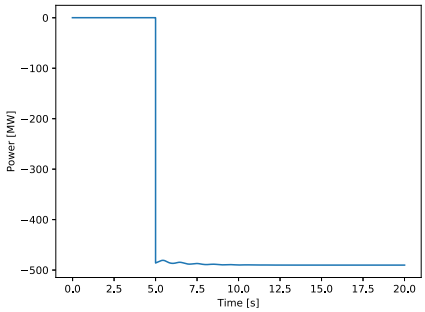

(d) Line 10-11.

Figure 4.1: Power flow when total load = 1000 MW and P_9 = 500 MW.

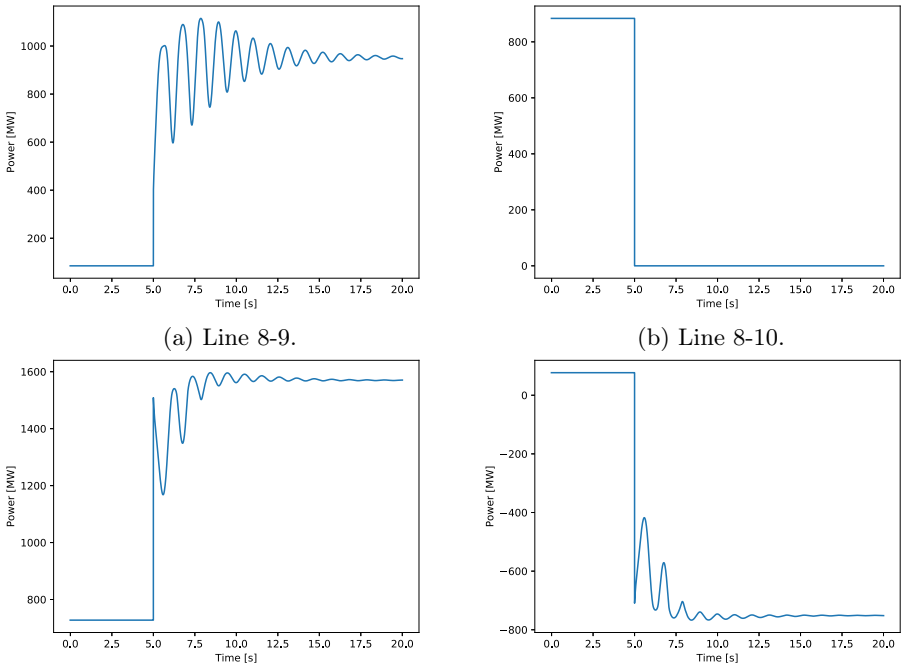

(a) Line 8-9.

(b) Line 8-10.

(c) Line 9-11.

(d) Line 10-11.

Figure 4.2: Power flow when total load = 1600 MW and P_9 = 500 MW.

Figure 4.1 and 4.2 shows how the power flow on the four lines of the 4-bus model changes after being subjected to a contingency of line 8-10 for two different operating states. When comparing the power flows of the two operating states it is clear that they are quite similar. The flow on line 8-9 and 10-11, the lines connecting the generators and the loads, goes from a value close to zero to carrying approximately half of the total load. The flow on line 9-11, the line connecting a generator and a load, is doubled. This is reasonable as the system is subjected to the same disturbance for both operating states. However, it can be seen that the case with a total load of 1600 MW experiences more oscillations than the case with a total load of 1000 MW. This is because an increase in total load moves the system closer to its stability limit, and hence the system is more stressed, and it becomes harder to stabilize at a steady-state value after the disturbance.

4.1.2 Rotor angle stability

4.1.2.1 Critical clearing time

The critical clearing time was investigated for the same operating states and contingency as the power flow. This is illustrated in fig. 4.3 and fig. 4.4. The figures show the electrical power and rotor angle of the generator buses for a stable clearing time (left) and an unstable clearing time (right). The blue curve represents bus 8 and the orange curve represents bus 9.

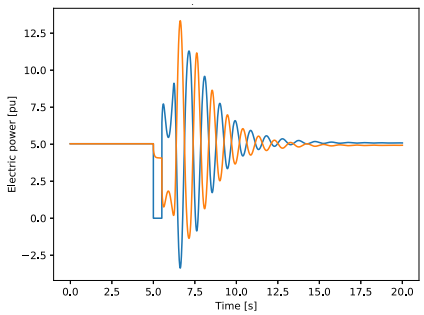

(a) Electrical power at $t_c = 510$ ms.

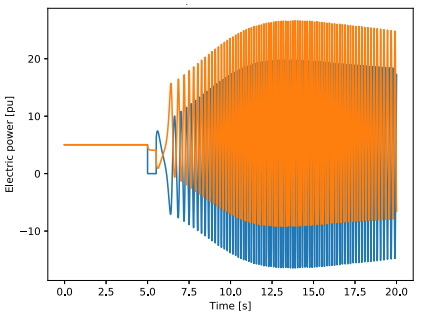

(b) Electrical power at $t_c = 520$ ms.

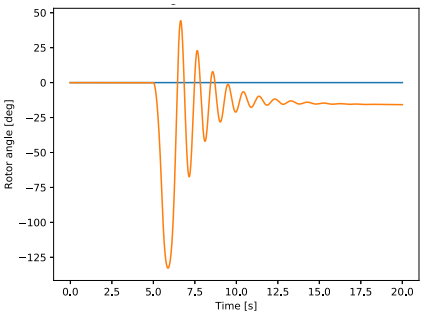

(c) Rotor angle at $t_c = 510$ ms.

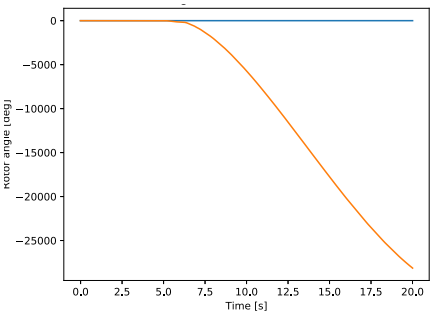

(d) Rotor angle at $t_c = 520$ ms.

Figure 4.3: Critical clearing time when total load = 1000 MW and $P_9 = 500$ MW.

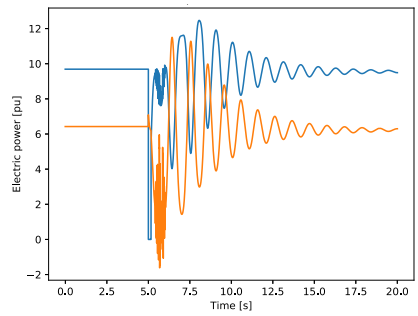

(a) Electrical power at $t_c = 160$ ms.

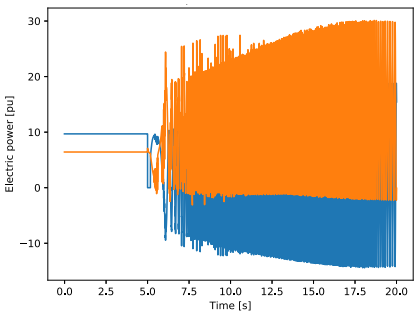

(b) Electrical power at $t_c = 170$ ms.

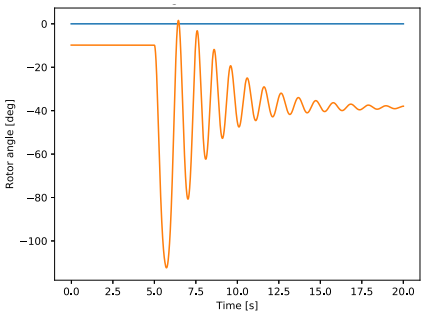

(c) Rotor angle at $t_c = 160$ ms

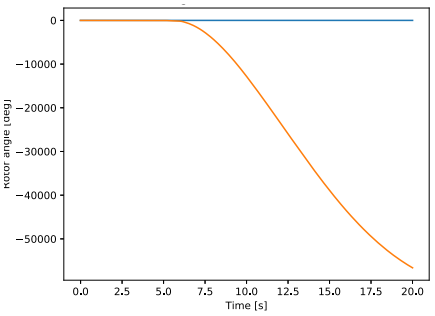

(d) Rotor angle at $t_c = 170$ ms.

Figure 4.4: Critical clearing time when total load = 1600 MW and $P_9 = 500$ MW.

The critical clearing time of the system was analyzed for different operating states. In fig. 4.3 and 4.4 the system response is illustrated when the clearing time exceeds the critical clearing time, and the system becomes unstable. This happens at $t_c = 520$ ms for the first operating state, and at $t_c = 170$ ms for the second operating state.

Figure 4.5 shows how the critical clearing time is affected by the generation at bus 8, and by the total load demand, when the system is subjected to a line fault and a contingency of the line connecting bus 8 and 10.

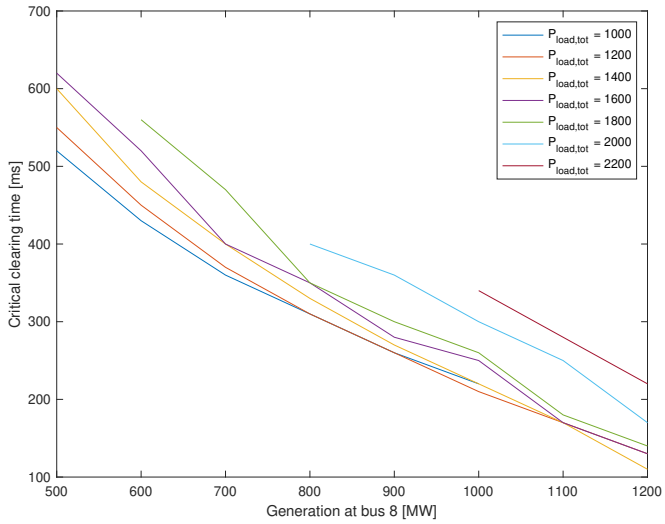

Figure 4.5: Critical clearing time as a function of P_8 for different values of total load.

In fig. 4.5, it can be seen that the generation at bus 8 has a more significant effect on the critical clearing time than the total load when the system is subjected to a disturbance on the line connecting bus 8 and 10. The figure shows that the critical clearing time for the system decreases as the production at bus 8 increases. When the production at bus 8 is increased, the power flow through bus 9 and towards the loads are also increased. As a result, the system is more loaded and therefore more vulnerable to a disturbance.

The rotor angle stability of the system will depend on the clearing time set for the simulation. For the operating states that were simulated, a clearing time of 100 ms would ensure that the rotor angle stability is not threatened. If the clearing time is set higher than 100 ms, the system will become unstable for high values of P_8.

4.1.3 Voltage stability

4.1.3.1 Voltage level

The voltage at the two load buses after the system was subjected to contingency 2 is shown in fig. 4.6 for the case without dynamic loads. The total load was set to 1600 MW and the production was set to 500 MW on bus 9. It can be seen that the voltage is below the defined limit of 0.9 p.u. at bus 10, and within the limits

at bus 11.

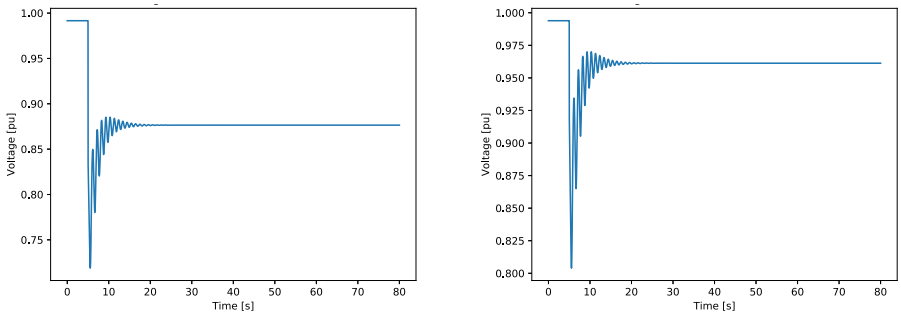

(a) Load 10. (b) Load 11.

Figure 4.6: Voltage in p.u. at the loads after contingency 2 when total load = 1600 MW and P_9 = 500 MW. Without dynamic loads.

Figure 4.7 presents the voltage at the two buses connected by the tap-changing transformer for both loads when the system was subjected to a contingency 2 for the case with dynamic loads. The total load was set to 1600 MW, and the generation at bus 9 was set to 500 MW. The blue curve represents the load side of the transformer, and the orange curve represents the grid side.

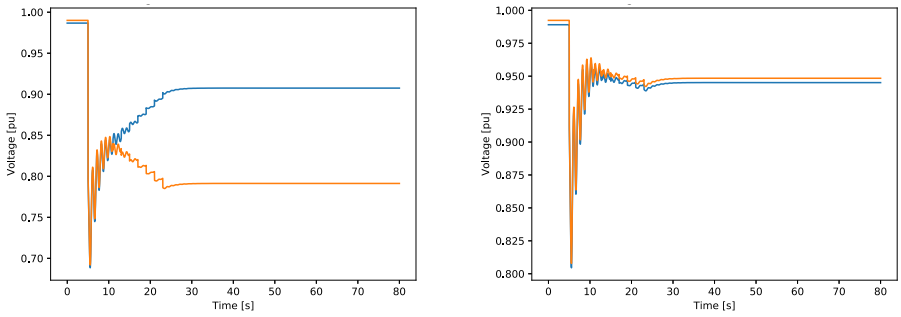

(a) Load 10. (b) Load 11.

Figure 4.7: Voltage in p.u. at the two buses that are connected to the tap-changing transformer for load 10 and load 11 when subjected to contingency 2.

The active power at the loads for the same operating state and disturbance is given in fig. 4.8.

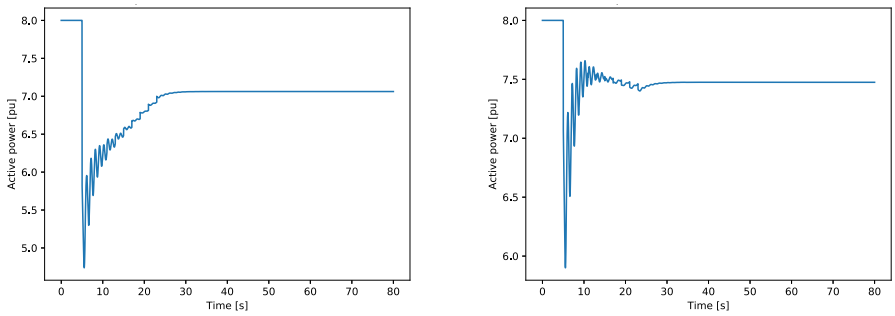

(a) Load 10

(b) Load 11.

Figure 4.8: Active power at load 10 and 11 in p.u. when subjected to contingecy 2.

In fig. 4.7 the voltage response when dynamic loads are implemented is shown. At bus 10, fig. 4.7a, it can be seen that the ratio at the transformer is adjusted in order to up-regulate the voltage to an acceptable level. In comparison, the voltage without dynamic loads, in fig. 4.6, stabilizes at a voltage level below the acceptable limit at bus 10. The figure also shows that the voltage at the grid side bus of the transformer is down-regulated. This is due to the ratio of the transformer; this voltage is down-regulated when the voltage at the load is up-regulated. This is a consequence of having dynamic loads that recover after being cut due to a too low voltage level. In fig. 4.8a, the time course of the active power for this exact case is given, and it can easily be seen how the load increases for each tap-change of the transformer. This causes extremely low voltage at the grid side of the transformer and increases the risk of voltage collapse. In other words, the system is more robust if the loads are voltage dependant.

The voltage at bus 11, fig. 4.7b, is not that affected by the current disturbance, and the voltage stabilized well within the acceptable limits. Nevertheless, it can be seen that the ratio of the transformer is adjusted such that the voltage is down-regulated a few levels. This is due to the load flow solution of the case. The time course of the active power at load 11 is given in fig. 4.8b. The altering in winding ratio of the transformer can also be seen in this figure.

4.1.3.2 PV-curves

In fig. 4.9, the voltage at bus 10 is plotted as a function of the total load for different values of P_8, creating several PV curves. Similarly, fig. 4.10 and fig. 4.11 shows the equivalent PV curves for the case with dynamic loads on the load side and grid side of the transformer, respectively.

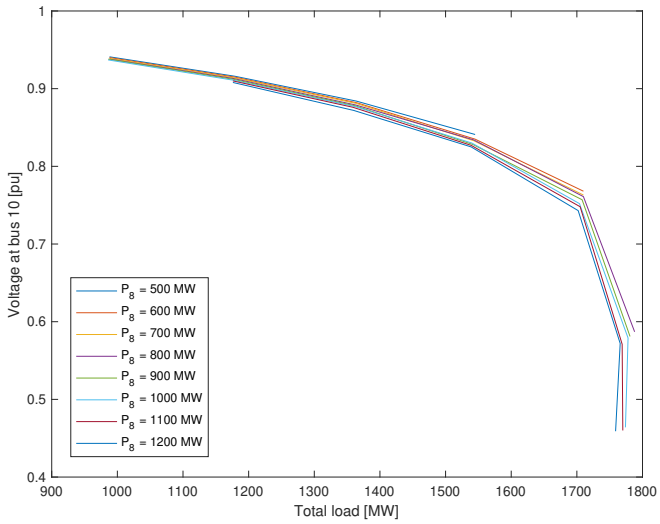

Figure 4.9: PV-curves for different values of P_8 for the case without dynamic loads.

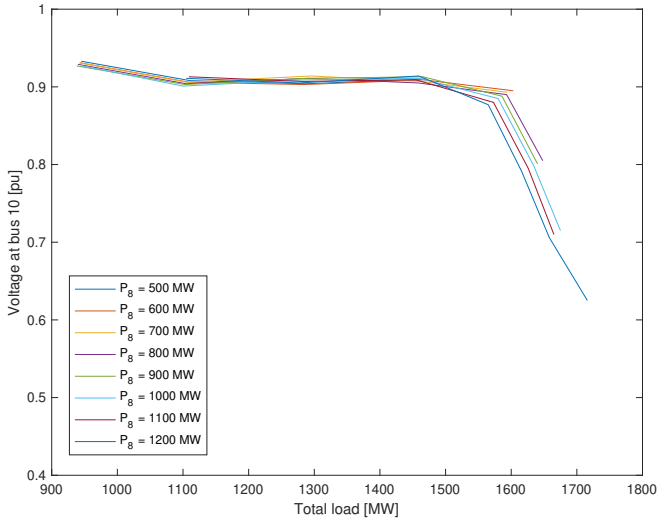

Figure 4.10: PV-curves for the bus at the load side of the tap-changing transformer for different values of P_8 for the case with dynamic loads.

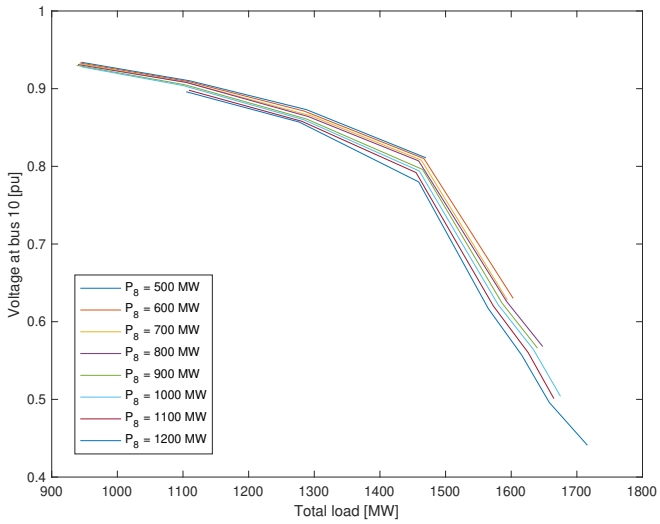

Figure 4.11: PV-curves for the bus at the grid side of the tap-changing transformer for different values of P_8 for the case with dynamic loads.

The PV-curve in fig. 4.9 shows that the voltage of bus 10 after contingency 2 decreases as the total load is increased. In comparison, the voltage on the load side of the transformer, shown in fig. 4.10 does not decrease significantly before it is close to the tip of the PV curve, where the critical point is located. However, the voltage on the grid side of the transformer, given in fig. 4.11, also has to be considered. These values start to decrease at approximately the same load as the case without transformer, but decrease more rapidly.

The three figures show that the limiting factor of the voltage stability of the system is the load. This is clear because the voltage is not very affected by how the production is divided between the two generators. For the case without dynamic loads and total load in excess of 1200 MW, the voltage stabilizes below the acceptable limit of 0.9 p.u. For the case with dynamic loads, the voltage limit is exceeded at the same load for most operating states. However, the voltage stabilized below the limit at this load if one the generators are carrying above 1000 MW. This has to be taken into consideration when the stability limits are decided.

4.1.4 Eigenvalue analysis

In fig. 4.12-4.14, the eigenvalues of the system after contingency 2 is given for different values of the controllers.

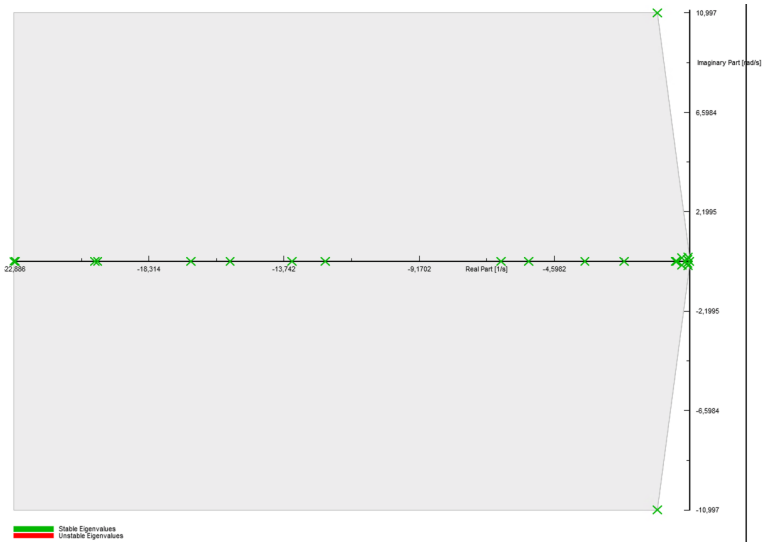

Figure 4.12: Eigenvalues post contingency of line 8-10 with base values of the controllers.

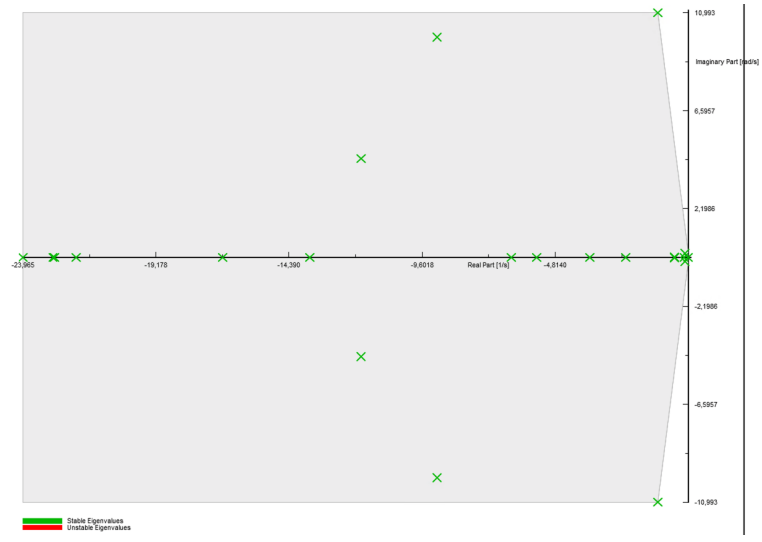

Figure 4.13: Eigenvalues post contingency of line 8-10 with adjusted values of the AVR.

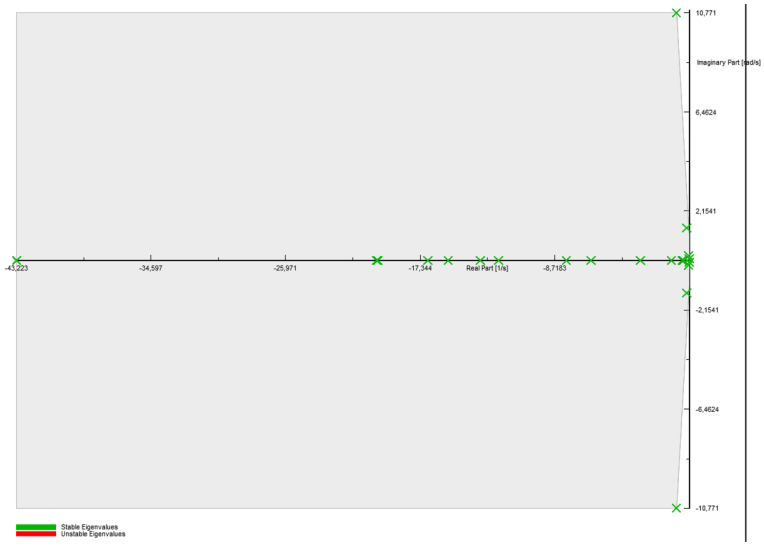

Figure 4.14: Eigenvalues post contingency of line 8-10 with adjusted values of the governor.

By measuring the natural frequency of the system, the electromechanical modes where found. All where complex conjugates, and table 4.1 lists the electromechanical mode with positive imaginary part for all three cases.

Table 4.1: The electromechanichal modes for different value of the controllers.

Mode	**Real part** [1/s]	**Imaginary part** [rad/s]	**Damped frequency** [Hz]	**Damping ratio**
Base	-1.1277	11.1204	1.7699	0.1009
Adjusted AVR	-1.1190	11.0274	1.7551	0.1010
Adjusted GOV	-0.9407	10.9070	1.7359	0.0859

The electromechanical modes can be found to be the ones with the largest imaginary part in the figures showing the eigenvalues. As the natural frequency is approximately the same for all cases, this is not especially affected by the change in values of the controllers. The damping ratio is also approximately the same for the case with adjusted values of the AVR and the base case, but it decreases for the case with adjusted values of the governor. Hence, the damping of the system is poorer when the values of the governor are adjusted. This can also be observed in the time responses of the system. These are given in fig. 4.15-4.17 for the different cases. The blue curves represent bus 8 and the organge curves represent bus 9.

The figures show the electric power of the generators when the system is subjected to contingency 2. The eigenvalues and the modes are obtained from PowerFactory, and the time responses are simulated in PyCont using PSS®E. This means that the time responses will not match completely with the eigenvalues, as the two softwares use different methods when performing the power system simulations.

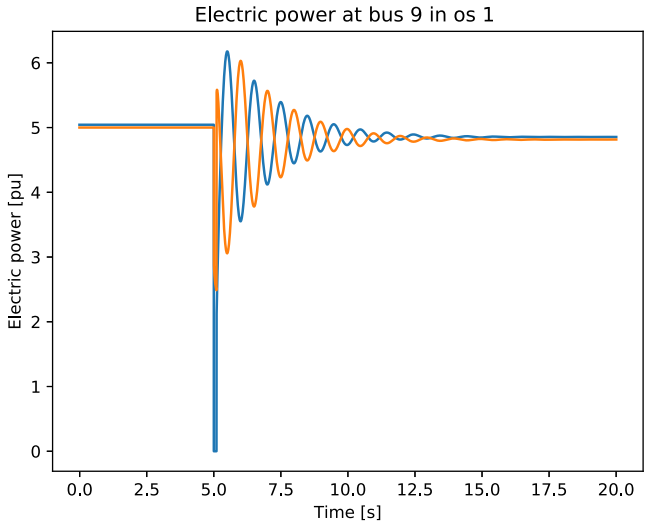

Figure 4.15: Electrical power of the two machines with base values of the controllers.

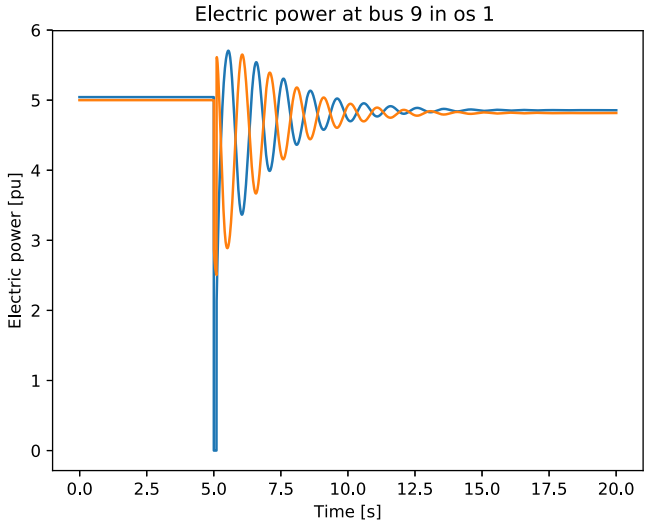

Figure 4.16: Electrical power of the two machines with adjusted values of the AVR.

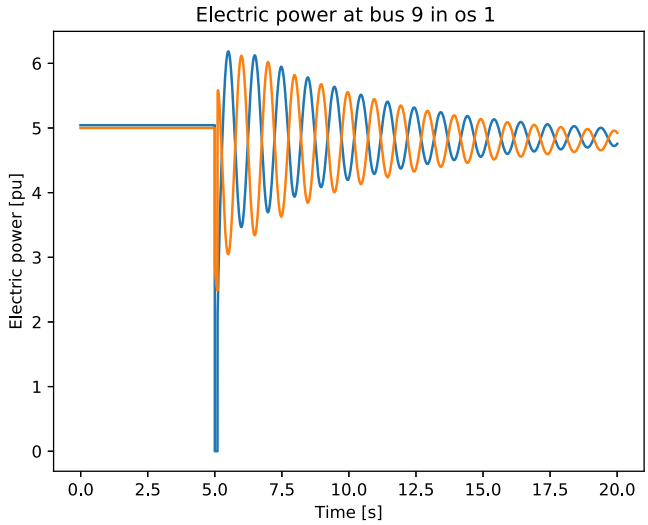

Figure 4.17: Electrical power of the two machines with adjusted values of the governor.

When the eigenvalue analysis was performed in PowerFactory, it was discovered how some of the parameters of the controllers affect the eigenvalues of the system. As the time constants in the AVR were decreased, the eigenvalues were more spread in the complex plane with more eigenvalues having larger imaginary parts. This will, according to [5], cause more oscillations of the time responses. However, these eigenvalues have larger real parts and are thus more damped. For this reason, they do appear in the time responses shown in fig. 4.12-4.14. They might however, appear in the response of other time variables.

When the temporary droop and the governor time constant of the turbine governor were decreased, several of the eigenvalues moved further into the left half-plane along the real axis. This caused them to be more damped, and thus they do not appear in the time response of the electrical power. It is only the electromechanical mode that affects the oscillations of the electric power. As the electromechanical mode moved closer to the imaginary axis, poorer damping is observed.

The eigenvalues of the system was also analyzed for a case with increased power flow on the lines, where the load were increased to 1600 MW and the production on bus 8 was increased to 1100 MW. The eigenvalues for this case post contingency of line 8-10 is given in fig. 4.18. The electromechanical modes for this case is slightly less damped than the base case. This is also observed in fig. 4.19, where the time response of the electric power of the machines is shown. This is expected, as it is common with less damped oscillations when the transferred power is increased.

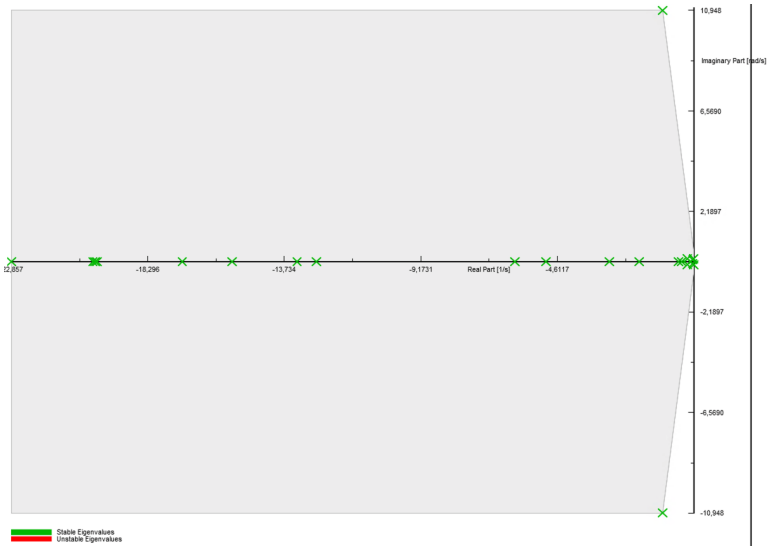

Figure 4.18: Eigenvalues post contingency of line 8-10 with increased flow on the lines.

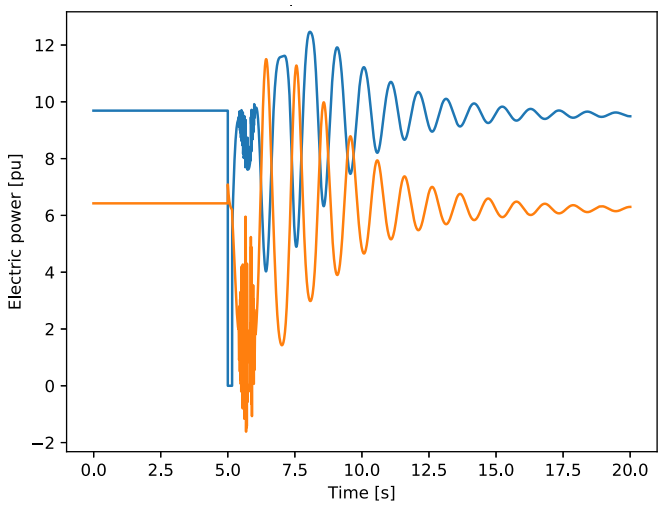

Figure 4.19: Electrical power of the two machines with increased power flow on the lines.

4.1.5 Transmission constraints based on stability analysis

When the voltage stability of the system was analyzed, it was discovered that the line connecting the load buses, line 10-11, is the limiting factor for the voltage stability. This is because it is the second load in the transmission that experiences unacceptable voltage values. Load 10 when line 8-10 is disconnected and load 11 when line 9-11 is disconnected. In section 4.1.3.2, it was discussed that voltage becomes unacceptable for load values above 1200 MW. It is assumed that the load is equally divided between the two load buses, and hence the line connecting the loads, line 10-11, should not carry more than 600 MW, and the transmission constraint on this line is set to this value. The operating state did also affect the voltage value some, and it was discussed that the system becomes more vulnerable when one of the generators are producing more than 1000 MW. To avoid stability issues related to this, the transmission constraint on the line connecting the two generator buses, line 8-9, is set to 1000 MW. The lines connecting the generator buses and the load buses, line 8-10 and 9-11, do not cause stability issues and are therefore not constrained in this case.

When deciding the transmission constraints, the rotor angle stability should also be considered. The effect of the critical clearing time was investigated and discussed in section 4.1.2.1. In order to evaluate the rotor angle stability, a clearing time has to be defined. A system like this can e.g., have a clearing time of 200 ms. This implies that the cases with a critical clearing time below this will cause instability in the power system if the system is subjected to a fault. The critical clearing time is mostly dependant on the distribution of the power generation, and hence all operating states with production higher than 1000 MW will cause instability. This matches the transmission constraints set with respect to the voltage stability.

4.1.6 Optimal power flow

The OPF problem was solved with the transmission constraints discussed above, and the objective function values were found for two values of the total load.

Table 4.2 shows the optimal operating states for two cases with a different value of the total load. The transmission constraint was set to 600 MW on line 10-11 and 1000 MW on line 8-9 based on the results from the voltage stability analysis and rotor angle stability analysis.

Table 4.2: Objective function for a total load of 1000 MW and 1200 MW with transmission constraints.

Total load [MW]	$\mathbf{P_8}$ [MW]	$\mathbf{P_9}$ [MW]	**Total losses** [MW]	**Objective function value** [$/h]
1000	285.88	714.50	0.387	14 296.78
1200	343.10	857.46	0.558	20 590.56

When comparing the optimal operating state for the same two cases without transmission constraints the exact same solutions were obtained. This is shown in table 4.3.

Table 4.3: Objective function for a total load of 1000 MW and 1200 MW without transmission constraints.

Total load [MW]	$\mathbf{P_8}$ [MW]	$\mathbf{P_9}$ [MW]	**Total losses** [MW]	**Objective function value** [$/h]
1000	285.88	714.50	0.387	14 296.78
1200	343.10	857.46	0.558	20 590.56

When investigating the optimal solution, it can be found that the power flow on the lines do not exceed the transmission constraints. Thus the OPF solution is equal with and without the the constraints. The majority of the power is transferred by the lines that are not constrained, and hence the transmission constrains had to be set much lower for it to be an issue in this case.

4.2 The Nordic 44 test system

4.2.1 Stability analysis

Throughout the dynamic simulations performed on the N44 model, it was observed that the main problem for the case studies was related to damping. There was no cases with problems related to voltage or frequency.

4.2.1.1 Case 0 - Base Case

When the system is operating at the base case, the flow between Eastern Norway and Sweden is divided between the two lines in the transmission. There is a total export from Norway to Sweden of approximately 1960 MW, 900 MW on line 1, and 1060 MW on line 2. When the system is subjected to a contingency of line 2 between Eastern Norway and Sweden, all flow between the two buses has to be carried by line 1. In fig. 4.20, it can be seen how the flow is affected by the contingency. The contingency causes oscillation that is damped after approximately 35 seconds. The flow on line 1 stabilizes at approximately 1792 MW after the disturbance.

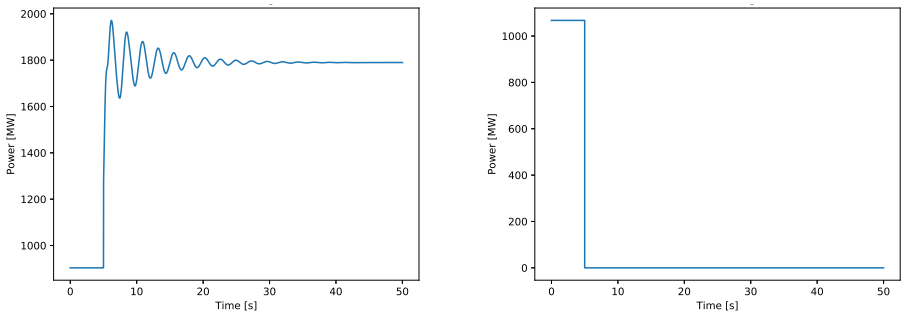

(a) Line 1 (b) Load 11.

Figure 4.20: Flow on the lines between Eastern Norway and Sweden at base case when the system is subjected to a contingency of line 2.

4.2.1.2 Case 1 - Increase production in Western Norway and load in Sweden

When the production at bus 5300 and 6100 in Western Norway, and the load at bus 3359 in Sweden were increased, the export to Sweden through bus 5101 also increased. This is shown in fig. 4.21. In addition, the system is poorly damped compared to the base case. This indicates that the system is operating closer to its stability limit.

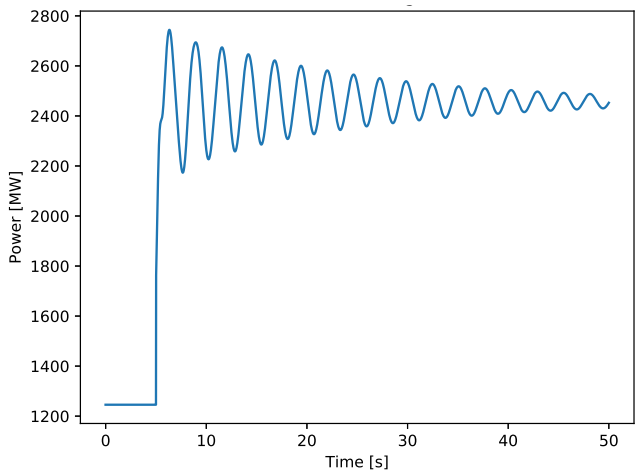

Figure 4.21: Power flow on line 1 between Eastern Norway and Sweden at case 1.

4.2.1.3 Case 2 - Decrease load in Oslo and production in Sweden

The export from Norway to Sweden increased when the load at bus 5400 and 5500, Oslo, and the production at bus 3115 were decreased. In fig. 4.22, the power flow of case 2.1, where the load in Oslo is reduced to 65% of the base value, and the production at bus 3115 in Sweden is reduced to 40%. The power flow on the specific line stabilized approximately 3200 MW for this case. Furthermore, the system also experiences a quite poor damping.

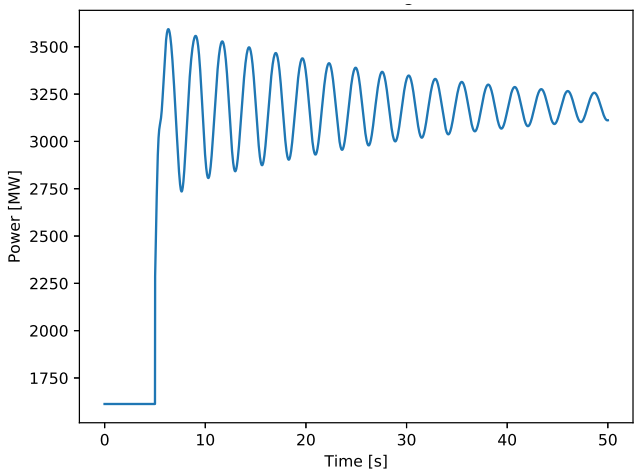

Figure 4.22: Power flow on line 1 between Eastern Norway and Sweden at case 2.1.

The power flow for case 2.2 is shown in fig. 4.23. In this case, the load in Oslo is reduced further on to 59% of the base value, and the production at bus 3115 is reduced to 30%. The damping of the system is even poorer for this case, and the results resemble standing waves.

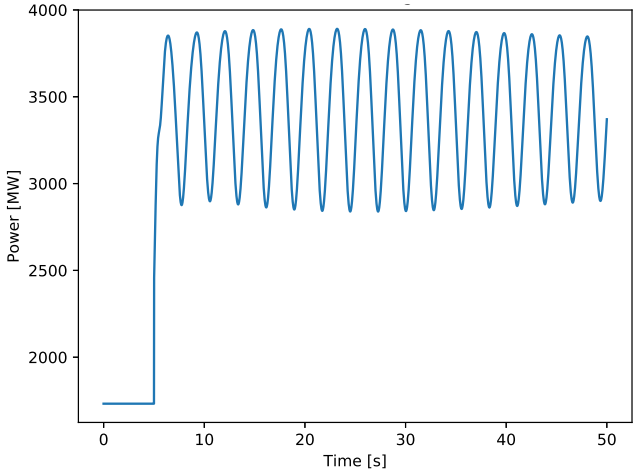

Figure 4.23: Power flow on line 1 between Eastern Norway and Sweden at case 2.2.

4.2.1.4 Case 3 - Increase production in Western Norway and decrease production in Finland

For case 3, the production in Western Norway was increased, and the production in Sweden was decreased. This also leads to an increase in export from Norway and Sweden through bus 5101. This is shown in fig. 4.24. Consequently, the power flows through this transmission and further on to Finland. The increase in the export leads to poorer damping and a more stressed system.

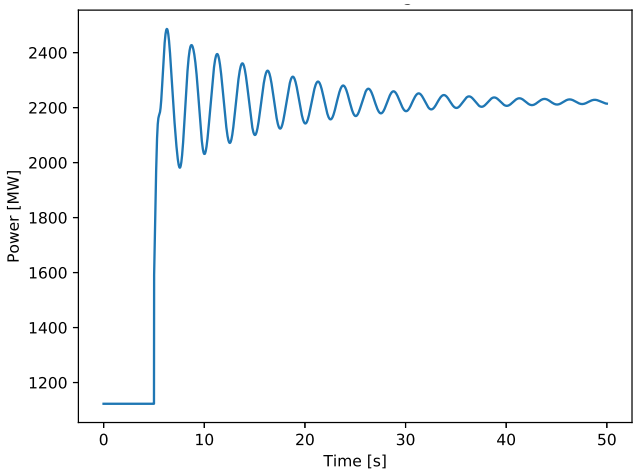

Figure 4.24: Power flow on line 1 between Eastern Norway and Sweden at case 3.

4.2.1.5 Case 4 - Increase production in Finland and load in Oslo

When the production in Finland and the load in Oslo were increased, the power export from Eastern Norway to Sweden decreased. The power flow on the specific line stabilizes approximately 1400 MW, and this can be seen in fig. 4.25. The power production in Noway has to cover the increased load in Oslo, and cannot export as much to Sweden as the base case. The missing power in Sweden due to lack of import from Norway has to be covered from other production, and for this case, it is likely to believe it is covered by the increased production in Finland.

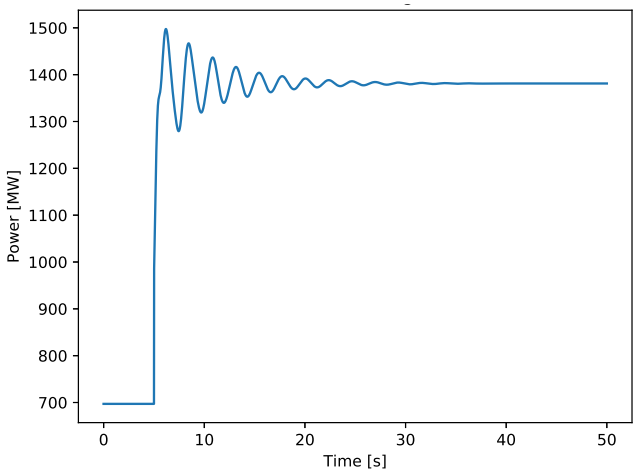

Figure 4.25: Power flow on line 1 between Eastern Norway and Sweden at case 4.

4.2.1.6 Case 5 - Decrease production in Finland and load in Oslo

For case 5, the production in Finland and the load in Oslo is decreased. This case is the opposite of case 4, and hence the power flow between Eastern Norway and Sweden is increased. This is shown in fig. 4.26. The power flow for this case is similar to case 2.1, where the load in Oslo also were decreased. This indicates that a power deficit in Sweden or Finland is covered by power from Norway through bus 5101.

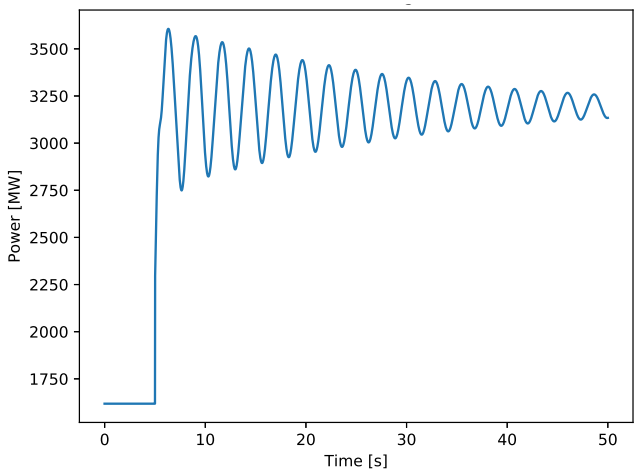

Figure 4.26: Power flow on line 1 between Eastern Norway and Sweden at case 5.

4.2.1.7 Case 6 - Increase production in Finland and load in Sweden

The last case investigates an increase in production in Finland and load in Sweden. Figure 4.27 shows a power flow quite similar to the base case. Hence, a change in production and loading in Sweden and Finland does not particularly affect the power flow and power exchange between Norway and Finland. In this case, it would probably be more interesting to investigate the power exchange between Finland and Sweden.

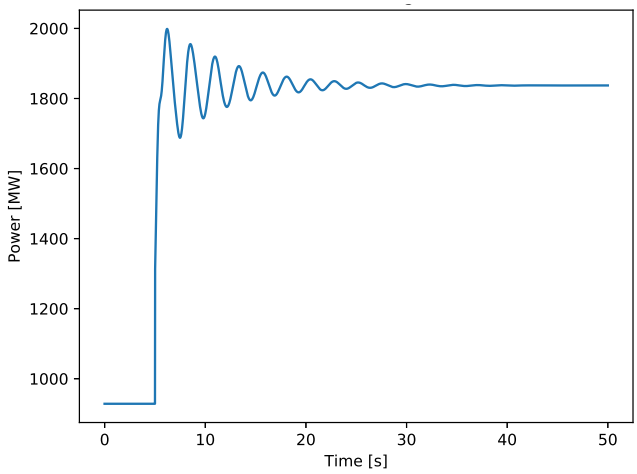

Figure 4.27: Power flow on line 1 between Eastern Norway and Sweden at case 6.

4.2.1.8 Transmission constraint on the line connecting Eastern Norway and Sweden based on stability analysis

In table 4.4, an overview of the power flow between Eastern Norway and Sweden, damping ratio, and the critical clearing time for the different cases are presented. The power flows are based on the results in fig. 4.20 - 4.27 above. The damping ratios are calculated by the method of logarithmic decrement [48]. The critical clearing times are found by simulating a short-circuit fault followed by a contingency of the line.

Table 4.4: Overview of power flow, damping ratio and critical clearing time for the different cases.

Case	**Power flow** [MW]	**Damping ratio**	**Critical clearing time** [ms]
0	1792	0.054	280
1	2465	0.022	110
2.1	3189	0.017	70
3	2224	0.034	150
4	1384	0.062	280
5	3200	0.019	80
6	1841	0.058	260

It can be seen that the flow on the line connecting Eastern Norway and Sweden increases as Norway experiences a power surplus and Sweden or Finland experiences a power deficit, and decreases for the opposite case. These observations indicate that a lot of power exchange between Norway and Sweden is through this specific transmission.

Both the damping ratio and the critical clearing time seems to be closely connected to the power flow. The relation between the damping ratio and the power flow is shown in fig. 4.28.

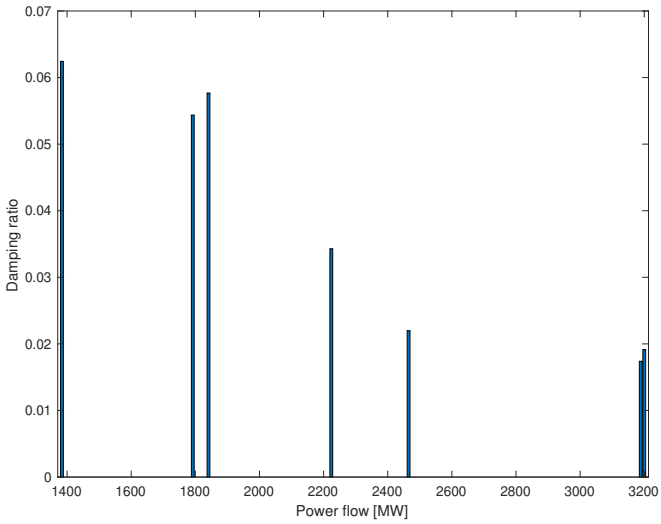

Figure 4.28: Damping ratio for different power flows.

The damping ratio decreases for increased power flow, with approximately 0.06 when the power flow is 1400 MW and approximately 0.02 when the power flow is 3200 MW. A system is considered adequately damped with a damping ratio above 0.05. A damping ratio of 0.05 corresponds to a power flow of approximately 1900 MW. Hence, the transmission constraint should be set to 1900 MW to ensure adequate damping. However, power systems can operate with damping down to 0.03, but a damping ratio lower than 0.03 has to be taken with caution. If the limit of the damping ratio is set to 0.03, the power flow will be constrained to approximately 2300 MW.

As discussed above, the critical clearing time of the system is also affected by the power flow. In fig. 4.29, the relation between critical clearing time and the power flow is shown.

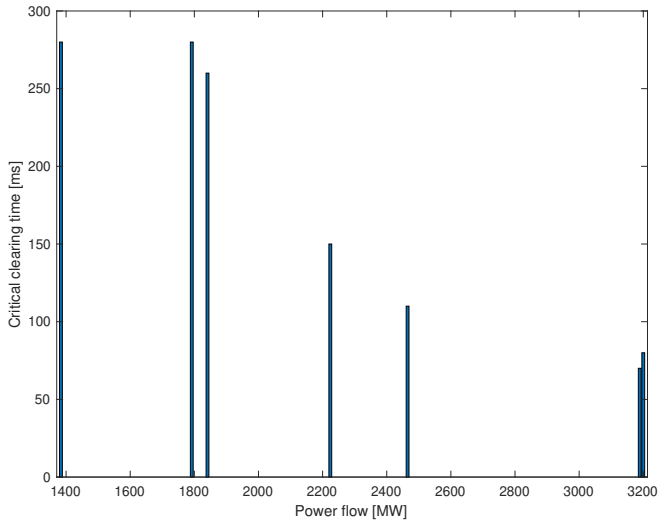

Figure 4.29: Critical clearing time for different power flows.

Similarly to the damping ratio, the critical clearing time also decreases with increased power flow. A low critical clearing time indicates that the system is operating close to the stability limit. In contrast, a high critical clearing time indicates a more robust system that is better prepared for a disturbance. By requiring a critical clearing time of min. 200 ms, the power flow will be constrained to approximately 2000 MW. However, if a critical clearing time of min. 150 ms, the transmission constraint can be set to approximately 2200 MW.

The simulations and analysis show that the damping and the critical clearing time are limiting factors when deciding the constraint on the line between Eastern Norway and Sweden. Where the transmission constraint is set depends on the requirements from the TSO. Based on the analysis performed in this thesis, it should not be set higher than 2200 MW. A transmission constraint of 2200 MW ensures a damping ratio above 0.03 and a critical clearing time of minimum 150 ms in the case of a contingency on one of the lines connecting Eastern Norway and Sweden.

4.2.2 Optimal power flow analysis

The OPF of the N44 test system was simulated for different transmission constraints on the line connection Eastern Norway and Sweden. In table 4.5, the change in production on the available machines are given for four different transmission constraints.

Table 4.5: Change in production at the available machines for different transmission constraints.

Bus	Transmission constraint of 3200 MW	Transmission constraint of 2400 MW	Transmission constraint of 1800 MW	Transmission constraint of 1000 MW
3000	5.20	156.40	276.82	477.48
3115	12.27	213.78	369.09	615.87
3249	39.34	491.33	832.51	1369.55
3300	21.21	263.64	453.54	590.40
5300	0	-127.64	-288.52	-502.64
5400	0	-156.02	-321.54	-539.66
5600	0	-27.10	189.04	-402.94
6100	-83.20	-949.50	-1301.10	-1778.1
7100	0	0	0	0

In table 4.5, it can be seen that the increased production is distributed on the available generators in Sweden, where bus 3249 accounts for a the biggest part. Bus 3249 is located in Northern Sweden and has a lot of capacity. The greatest amount of demand is in Southern Sweden where the largest cities are located. It is cheaper to increase the production close to the load to avoid cost related to line losses. As the price in Sweden is equal for all of the generators, it is reasonable that the increased production is spread around the country to cover the deficit that occurred when the import was decreased close to the demand. However, the production in Southern Sweden is limited, and it is therefore reasonable that the demand is covered by production in Northern Sweden where the capacity is high.

The decrease in production is at the buses in Norway, as the export to Sweden decreases with a decreased transmission constraint. Bus 6100, located in Western Norway, accounts for the greatest decrease in production. The price for production is, like in Sweden, equal for every generation unit in Norway. Hence, it is reasonable that the production in Western Norway is decreased, as this reduces losses. In addition, the greatest amount of the production is located in Western Norway, which can easily handle the decrease production. During the case studies, it was observed that an increase in production in Western Norway caused an increase in export to Sweden. A decrease in production to reduce the flow to Sweden is therefore reasonable.

The production is also decreased at bus 5400, which is located in Eastern Norway and close to the export line. It is reasonable to believe that the production on bus 5400 contributes to the export in Sweden.

The objective function value for the different transmission constraints was also calculated. In fig. 4.30, the relation between increase in objective function value and the transmission constraint is illustrated.

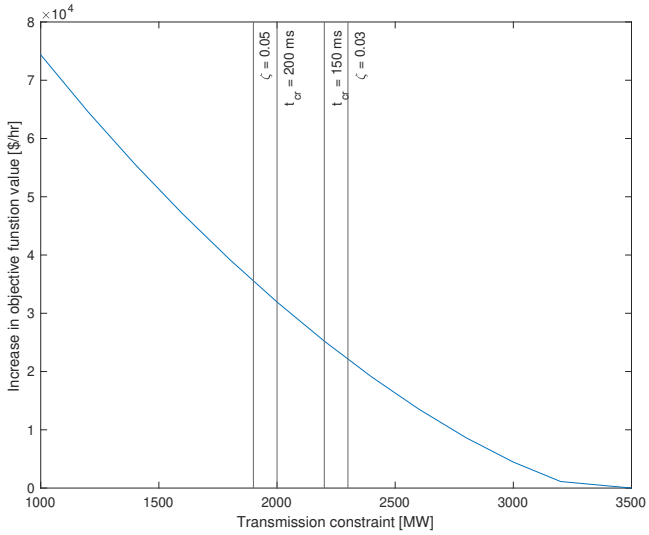

Figure 4.30: Increase in objective function value as a function of the transmission constraint. The proposed constraints are marked for different values of damping ratio, ζ, and, critical clearing time, t_{cr}.

Figure 4.30 shows that the objective function value, and hence the operating cost, increases with a decreased transmission constraints. The starting point is set to the objective function value for the case without constraints. This way, the graph shows the cost of implementing a transmission constraint of the line connecting Eastern Norway and Sweden. The relation between the cost and the constraint indicates that it is more expensive to operate with conservative constraints.

When the damping of the system was discussed, two values for the transmission constraint were proposed. The most conservative constraint was 1900 MW with a requirement of minimum 0.05 damping. A transmission constraint of 1900 MW would lead to an increased cost of approximately 35 000 \$/hr. In comparison, the less conservative constraint of 2300 MW when requiring a minimum of 0.03 damping, would cause an increase of approximately 22 000 \$/hr in objective function value. It is thus quite large costs related to the transmission constraints, especially with strict requirements.

Similar results were observed when investigating the proposed transmission constraints based on the critical clearing time. When requiring a critical clearing time above 200 ms, the transmission constraint was set to 2000 MW. The increase in objective function value is approximately 32 000 \$/hr with a transmission constraint of 2000 MW. Furthermore, the transmission constraint was set to 2200 MW when requiring a critical clearing time of 150 ms. A transmission constraint of 2200 MW

corresponds to an increased cost of approximately 25 000 $/hr.

4.2.2.1 Reliability

In the specialization project [16], it was observed that the optimum of the OPF was more affected by the transmission constraints when the load was high and the transmission lines were more loaded. It was discussed that it was more important for the TSO to set good constraints in order to utilize the grid optimally in these situations. It can be challenging to decide how conservative the constraints should be set. Too conservative constraints do not utilize the available capacity in the system, and this can be expensive in situations with high loading. Nevertheless, non-conservative constraints can, in the worst case, lead to fatal consequences, like blackouts. Reliability analysis can be a useful tool in these kinds of situations. In reliability analysis, the reliability of supply indices is decided [23]. The most important supply indices that can be interesting to investigate are, frequency and duration of simulations, and interruption costs.

The interruption cost can be analyzed as a function of the transmission constraints that are studied in this thesis. It is reasonable to think that high transmission constraints can lead to high interruption costs. This is because a blackout is more likely if more power is transferred over the lines. Furthermore, an interruption on a line will give greater consequences in lost load if there is more power transferred over the lime. Oppositely, the interruption cost will be lower if the constraint is set very conservatively. By determining a maximum acceptable interruption cost, the maximum transmission capacity can be decided. By performing a reliability analysis, the interruption cost can be found for different values of the transmission constraint. This way the optimal solution between the operating costs and the interruption costs can be calculated.

The reliability also aims to answer three fundamental questions [15]:

- What may go wrong?
- How likely is it that something may go wrong?
- What are the consequences?

Problems related to reliability and interruption costs can be caused by badly set transmission constraints. The consequences of bad constraints can be that the capacity is not adequately utilized for conservative constraints or overload on the lines for non-conservative constraints. Too conservative constraints will lead to challenges in operation in the case of high loads. This is because it might be difficult to supply all of the load if the capacity of the system is not adequately utilized. It can also lead to higher operating cost and price differences between

price areas if expensive production has to cover the demand in deficit areas rather than the demand being covered by import. In the opposite situation, with non-conservative constraints, a blackout can occur due to overloading on a transmission line. That will cause consumers to end up without power. A blackout is also very expensive for the system operators.

The dynamic simulation that was performed is a helpful tool when deciding the transmission constraints. For the contingencies that were simulated, it is possible to set the transmission constraints such that stability issues are avoided. However, every possible fault was not simulated, so there may occur situations where the stability limits are violated if other components are lost.

5 Conclusion

When the dynamic simulations were performed on the 4-bus model, it was discovered that the voltage was the limiting factor. The transmission constraints were decided to ensure voltage at acceptable limits for every operating state with N-1 security. The optimal power flow simulations showed that the transmission constraints did not affect the cost at optimum under normal operations, as the power flow of the constrained lines did not exceed the limits. By using the transmission constraints that were decided from the result of the dynamic simulation, the solution of the optimal power flow simulations will be acceptable for all operating states with N-1 security.

Similar simulations were performed on the Nordic 44 test system when a contingency on one of the lines connecting Easter Norway and Sweden occurred. It was discovered that the limiting factors related to stability was the damping and the critical clearing time. The damping and the critical clearing time were both decreased for increased power flow. By simulating the OPF for different transmission constraint, it was found that the operating cost increased when the transmission constraint was decreased. Hence, it is more expensive to operate with conservative constraints.

5.1 Further work

Based on the work in this thesis, the following list gives some suggestion for further work:

- Investigate the power flow and stability limits on more lines connecting the Nordic countries or the price areas within the Nordic power system.
- Integrate reliability analysis with the OPF analysis to investigate how important it is to set good constraint.
- Perform more extensive stability analysis on the N44 model or a more advanced grid model.

Bibliography

[1] D. A. Douglass et al. “A Review of Dynamic Thermal Line Rating Methods With Forecasting”. In: *IEEE Transactions on Power Delivery* 34.6 (2019), pp. 2100–2109.

[2] Agder Energi. *Spenningskvailtet*. 2015. URL: https://www.aenett.no/virksomhet/spenningskvalitet/ (visited on 03/30/2020).

[3] A. Arif et al. “Load Modeling—A Review”. In: *IEEE Transactions on Smart Grid* 9.6 (2018), pp. 5986–5999.

[4] R. Bacher. *Class text ETH Zürich "SmartGrids: System Optimization of liberalized electric power system"*. Version May 3, 2012. ETH Zürich, 2012.

[5] J. G. Balchen, T. Andresen, and B. A. Foss. *Reguleringsteknikk*. 6th ed. Institutt for teknisk kybenetikk, NTNU, 2016.

[6] K. [den Bergh] et al. “Redispatching in an interconnected electricity system with high renewables penetration”. In: *Electric Power Systems Research* 127 (2015), pp. 64–72. ISSN: 0378-7796. DOI: https://doi.org/10.1016/j.epsr.2015.05.022. URL: http://www.sciencedirect.com/science/article/pii/S0378779615001637.

[7] F. Capitanescu et al. “State-of-the-art, challenges, and future trends in security constrained optimal power flow”. In: *Electric Power Systems Research* 81 (Aug. 2011), pp. 1731–1741. DOI: 10.1016/j.epsr.2011.04.003.

[8] S. Chakrabarti. “Static load modelling and voltage stability indices”. In: *International Journal of Power and Energy Systems* 29 (Jan. 2009). DOI: 10.2316/Journal.203.2009.3.203-4336.

[9] DIgSILENT. *PowerFactory Applications*. URL: https://www.digsilent.de/en/powerfactory.html (visited on 04/15/2020).

[10] Y. Dvorkin et al. “Optimizing Primary Response in Preventive Security-Constrained Optimal Power Flow”. In: *IEEE Systems Journal* 12.1 (2018), pp. 414–423.

[11] H. Emani and J. A. Sadri. “Congestion management of transmission lines in the market environment”. In: *International Research Journal of Applied and Basic Sciences* 3 (2012), pp. 2572–2580.

[12] Energi Norge. *Forsyningssikkerhet og beredskap*. URL: https://www.energinorge.no/fagomrader/strommarked/kraftsystemet/forsyningssikkerhet-og-beredskap/ (visited on 05/08/2020).

[13] Energifakta Norge. *Strømnettet*. URL: https://energifaktanorge.no/norsk-energiforsyning/kraftnett/ (visited on 05/08/2020).

[14] Energifakta Norge. *The Power Market*. 2017. URL: https://energifaktanorge.no/en/norsk-energiforsyning/kraftmarkedet/ (visited on 05/25/2020).

[15] O. Gjerde et al. "Enhanced method for reliability of supply assessment - an integrated approach". In: *2016 Power Systems Computation Conference (PSCC)*. 2016, pp. 1–7.

[16] M. Haaland. *Stability limits and uncertainty in power system optimization*. Project report in TET4520. Department of Electric Power Engineering, NTNU – Norwegian University of Science and Technology, Dec. 2019.

[17] K. E. Holbert and G. T. Heydt. "Prospects for dynamic transmission circuit ratings". In: *ISCAS 2001. The 2001 IEEE International Symposium on Circuits and Systems (Cat. No.01CH37196)*. Vol. 3. 2001, 205–208 vol. 2.

[18] K. M. Hovland. *Derfor ble strømmen dyr*. URL: https://www.tu.no/artikler/derfor-ble-strommen-dyr/239161 (visited on 04/27/2020).

[19] "IEEE Standard Requirements for Tap Changers". In: *IEEE Std C57.131-2012 (Revision of IEEE Std C57.131-1995)* (May 2012), pp. 1–73.

[20] S. H. Jakobsen. *N44 version by Sigurd*. URL: https://figshare.com/articles/N44_version_by_Sigurd/7466630 (visited on 04/27/2020).

[21] S. H. Jakobsen. *psse$_m$odels*. 2019. URL: https://github.com/Hofsmo/psse_models (visited on 05/11/2020).

[22] S. Jakobsen and E. Solvang. *The Nordic 44 test network*. Tech. rep. Dec. 2018. DOI: 10.6084/m9.figshare.7464386.v1.

[23] G. H. Kjølle and O. Gjerde. *The OPAL methodology for reliability analysis of power systeme*. Tech. rep. 2012.

[24] P. Kumkratug. "Power-Voltage Characteristics of Power System with the Short Transmission Line". In: *Americal Journal of Applied Sciences* 6.9 (2012), pp. 906–908.

[25] P. Kundur et al. "Definition and classification of power system stability IEEE/CIGRE joint task force on stability terms and definitions". In: *IEEE Transactions on Power Systems* 19.3 (2004), pp. 1387–1401.

[26] J. Machowski, J. W. Bialek, and J. R. Bumby. *Power System Dynamics - Stability and Control*. 2nd ed. Wiley, 2008.

[27] MATPOWER. *About MATPOWER*. URL: https://matpower.org/about/ (visited on 04/07/2020).

[28] MATPOWER. *psse2mpc*. URL: https://matpower.org/docs/ref/matpower5.0/psse2mpc.html (visited on 05/27/2020).

[29] Matpower. *Runopf*. 2005. URL: https://matpower.org/docs/ref/matpower5.0/runopf.html (visited on 05/10/2020).

[30] Nord Pool. *About Us*. URL: https://www.nordpoolgroup.com/About-us/ (visited on 05/25/2020).

[31] NordPool. *Bidding areas*. URL: https://www.nordpoolgroup.com/the-power-market/Bidding-areas/ (visited on 05/25/2020).

[32] Qisheng Liu, Yunping Chen, and Dunfeng Duan. "The load modeling and parameters identification for voltage stability analysis". In: *Proceedings. International Conference on Power System Technology*. Vol. 4. 2002, 2030–2033 vol.4.

[33] H. Saadat. *Power System Analysis*. 3rd ed. PSA Publishing, 2010.

[34] ScienceDirect. *Transmission System Operator*. URL: https://www.sciencedirect.com/topics/engineering/transmission-system-operator (visited on 05/25/2020).

[35] Siemens. *Application Program Interface (API) Manual*. 2018.

[36] Siemens. *Eigenvalue Analysis PSS®E Product Suite*. 2018. URL: https://www.scribd.com/document/440927475/Eigenvalue-Analysis-PSSE-pdf (visited on 01/04/2020).

[37] Siemens. *Model Library*. 2018.

[38] Siemens. *Providing an industry benchmark for simulation results*. URL: https://new.siemens.com/global/en/products/energy/services/transmission-distribution-smart-grid/consulting-and-planning/pss-software/pss-e.html (visited on 04/15/2020).

[39] SINTEF. *Generally Accepted Reliability Principle with Uncertainty modelling and through probabilistic Risk assessment*. URL: https://www.sintef.no/projectweb/garpur (visited on 11/19/2019).

[40] SINTEF. *HILP - Analyse av ekstraordinære hendelser i kraftnettet*. 2016. URL: https://www.sintef.no/prosjekter/hilp/ (visited on 11/18/2019).

[41] J. Slootweg et al. "A study of the eigenvalue analysis capabilities of power system dynamics simulation software". In: (June 2002).

[42] E. H. Solvang. "Dynamic Simulations of Simulataneous HVDC Contingencies in the Nordic Power System Considering System Integrity Protection Schemes". MA thesis. NTNU – Norwegian University of Science and Technology, 2018.

[43] Statnett. *Dagens løsninger i systemdriften*. Tech. rep. 2016. DOI: https://www.statnett.no/globalassets/for-aktorer-i-kraftsystemet/systemansvaret/om-systemansvaret/dagens-losninger-i-systemdriften-2016.pdf.

[44] Statnett. *Tall og data fra kraftsystemet, Nordisk kraftflyt*. URL: https://www.statnett.no/for-aktorer-i-kraftbransjen/tall-og-data-fra-kraftsystemet/ (visited on 05/25/2020).

[45] D. Trudnowski, D. Kosterev, and J. Undrill. "PDCI damping control analysis for the western North American power system". In: *2013 IEEE Power Energy Society General Meeting*. 2013, pp. 1–5.

[46] Y. Wang et al. "Intelligent control of on-load tap changer of transformer". In: *2011 1st International Conference on Electric Power Equipment - Switching Technology*. Oct. 2011, pp. 178–181. DOI: 10.1109/ICEPE-ST.2011.6122963.

[47] I. Wangensteen. *Power System Economics - the Nordic Electricity Market*. 2nd ed. Fagbokforlaget, 2012.

[48] Wikipedia. *Logarithmic decrement*. URL: https://en.wikipedia.org/wiki/Logarithmic_decrement (visited on 06/20/2020).

[49] N. I. Yusoff, A. A. M. Zin, and A. Bin Khairuddin. "Congestion management in power system: A review". In: *2017 3rd International Conference on Power Generation Systems and Renewable Energy Technologies (PGSRET)*. 2017, pp. 22–27.

[50] Y. G. Zeng, G. Berizzi, and P. Marannino. "Voltage stability analysis considering dynamic load model". In: *1997 Fourth International Conference on Advances in Power System Control, Operation and Management, APSCOM-97. (Conf. Publ. No. 450)*. Vol. 1. 1997, 396–401 vol.1.

A Network data of the 4-bus model

This appendix includes the network data of the 4-bus models used in this thesis.

A.1 4-bus model

The network data for the 4-bus network is given in this section. The bus data is given in table A.1, the branch data in table A.2, the generation data in table A.3, and the generation cost data in table A.4.

Table A.1: Bus data.

Bus no.	**Type**	$\mathbf{P_d}$	$\mathbf{Q_d}$	$\mathbf{G_s}$	$\mathbf{B_s}$	**Area**	$\mathbf{V_m}$	$\mathbf{V_a}$	**baseKV**	**Zone**	$\mathbf{V_{max}}$	$\mathbf{V_{min}}$
8	3	0	0	0	0	1	1	0	420	1	1.1	0.9
9	2	0	0	0	0	1	1	0	420	1	1.1	0.9
10	1	50	0	0	0	1	1	0	420	1	1.1	0.9
11	1	50	0	0	0	1	1	0	420	1	1.1	0.9

Table A.2: Branch data.

From bus	**To bus**	**r**	**x**	**b**	**rateA**	**rateB**	**rateC**	**ratio**	**angle**	**status**
8	9	0.000860882	0.05	0	40	40	40	0	0	1
8	10	0.000860882	0.002343076	0	0	0	0	0	0	1
9	11	0.000860882	0.002343076	0	0	0	0	0	0	1
10	11	0.000860882	0.05	0	40	40	40	0	0	1

Table A.3: Generator data.

Bus	$\mathbf{P_g}$	$\mathbf{Q_g}$	$\mathbf{Q_{min}}$	$\mathbf{Q_{max}}$	$\mathbf{V_g}$	**mBase**	**status**	$\mathbf{P_{max}}$	$\mathbf{P_{min}}$
8	-	0	986	-986	1	1357	1	1230	0
9	-	0	986	-986	1	1357	1	1230	0

Table A.4: Generator cost data.

Model	**Startup**	**Shutdown**	**n**	$\mathbf{c_2}$	$\mathbf{c_1}$	$\mathbf{c_0}$
2	0	0	3	0.05	0	0
2	0	0	3	0.02	0	0

A.2 4-bus model with dynamic loads

The case including dynamic loads are very similar to the 4-bus network, and hence the generation data, generation cost data and branch data is equal and given in appendix A.1. The bus data is however slightly changed, and given in table A.5. The transformer data is new for this case, and given in table A.6.

Table A.5: Bus data.

Bus no.	**Type**	**P_d**	**Q_d**	**G_s**	**B_s**	**Area**	**V_m**	**V_a**	**baseKV**	**Zone**	**V_{max}**	**V_{min}**
8	3	0	0	0	0	1	1	0	420	1	1.1	0.9
9	2	0	0	0	0	1	1	0	420	1	1.1	0.9
10	1	0	0	0	0	1	1	0	420	1	1.1	0.9
11	1	0	0	0	0	1	1	0	420	1	1.1	0.9
1001	1	500	0	0	0	1	1	0	230	1	1.1	0.9
1101	1	500	0	0	0	1	1	0	230	1	1.1	0.9

Table A.6: Bus data.

From bus no.	**To bus no.**	**Controlled bus**	**Control mode**	**Specified R**	**Specified X**	**Rmax**	**Rmin**	**Vmax**	**Vmin**
10	1001	1001	Voltage	0.00	0.01	1.3	0.7	1.1	0.9
11	1101	1101	Voltage	0.00	0.01	1.3	0.7	1.1	0.9

B | Dynamic data for the 4-bus model

This appendix includes the data of the dynamic PSS®E 4-bus models used in this thesis.

B.1 4-bus model

The dynamic data of the 4-bus network is provided in this section. The generator controller is of the type GENSAL with the dynamic data given in table B.1, the exciter is of the type SCRX with the dynamic data in table B.2 and the turbine governor is of the type HYGOV with the dynamic data in table B.3.

	Value	**Description**
1	10,1300	T'_{d0} (> 0)
2	0,0600	T''_{d0} (> 0)
3	0,1000	T''_{q0} (> 0)
4	4,5430	Inertia H
5	0,0000	Speed Damping D
6	1,0360	X_d
7	0,6300	X_q
8	0,2800	X'_d
9	0,2100	$X''_d = X''_q$
10	0,1154	X_1
11	0,1024	S(1.0)
12	0,2742	S(1.2)

Table B.1: GENSAL Dynamic Data.

	Value	Description
1	0,2539	TA/TB
2	13,0000	TB (> 0)
3	31,0000	K
4	0,0500	TE
5	0,000	EMIN
6	4,0000	EMAX
7	0,0000	CSWITCH (0=bus-feb, 1=solid-fed)
8	0,0000	rc/rfd

Table B.2: SCRX Dynamic Data.

	Value	Description
1	0,0600	R, Permanent Droop
2	0,4000	r, Temporary Droop
3	5,0000	T_r(> 0) Governor Time Constant
4	0,0500	T_f(> 0) Filter Time Constant
5	0,2000	T_g(> 0) Servo Time Constant
6	0,1000	VELM, Gate Velocity Limit
7	1,0000	GMAX, Maximum Gate Limit
8	0,0000	GMIN, Minimum Gate Limit
9	1,0000	T_W(> 0) Water Time Constant
10	1,1000	A_t, Turbine Gain
11	0,5000	D_{turb}, Turbine Damping
12	0,1000	qNL, No Load Flow

Table B.3: HYGOV Dynamic Data.

B.2 4-bus model with dynamic load

The 4-bus network with the dynamic load includes the same generator controllers, exciters and turbine governers as the network without dynamic load, and hence the dynamic data is given in appendix B.1. This section provides the dynamic data of the OLTC1T transformers. This is presented in table B.4.

	Value	Description
1	5,0000	Td, Timed delay (sec.)
2	1,0000	TC, Time constant for shift mechanism (sec.)
3	2,0000	TSD, Time before sending subsequent signal (sec.)

Table B.4: OLTC1T Dynamic Data.

C | Code used for dynamic simulations on the N44 test system

```
import os

import matplotlib.pyplot as plt

import psse34
import psspy
import dyntools
import redirect
import csv

plotting = 1
case_1 = 0  # Increase production in Western Norway and load
# in Sweden
case_2 = 0  # Decrease load in Oslo and production in Sweden
case_3 = 0  # Increase production in Western Norway and
# decrease production in Finland
case_4 = 0  # Increase load in Oslo and production in
# Finland
case_5 = 0  # Decrease load in Oslo and production in
# Finland
case_6 = 1  # Increase load in Sweden and production in
# Finland

voltage_stability = 1
frequency_stability = 0
rotor_angle_stability = 0

# Define default PSS/E variables
_i = psspy.getdefaultint()
_f = psspy.getdefaultreal()
_s = psspy.getdefaultchar()

# Redirect the PSS/E output to the terminal
redirect.psse2py()

```

```
36 psspy.throwPssExceptions = True
37
38 # Files and folders
39 cwd = os.getcwd()  # Get the current directory
40 models = os.path.join(cwd, "Models")  # Name of the folder
41 # with the models
42
43 # Names of the case files
44 casefile = os.path.join(models, "Scenario1.sav")
45 dyrfile = os.path.join(models, "Scenario1.dyr")
46
47 # Load bus file
48 load_buses = []
49 with open('delivery_points_n44.csv', 'rb') as csvfile:
50     reader = csv.reader(csvfile)
51     for row in reader:
52         load_buses.append(int(row[0]))
53
54 # Gen bus file
55 gen_buses = []
56 with open('machines.csv', 'rb') as csvfile:
57     reader = csv.reader(csvfile)
58     for row in reader:
59         gen_buses.append(int(row[0]))
60
61 # Name of the file where the dynamic simulation output is
62 # stored
63 outputfile = os.path.join(cwd, "output.out")
64
65 # Start PSS/E
66 psspy.psseinit(10000)
67
68 # Initiation ------------------------------------------------
69 psspy.case(casefile)  # Read in the power flow data
70 psspy.dyre_new([1, 1, 1, 1], dyrfile, "", "", "")
71
72 # Change the power flow
73 if case_1:
74     # Change production in western Norway
75     # Sima
76     psspy.machine_chng_2(5300, r"""1""",
77                          [_i, _i, _i, _i, _i, _i],
78                          [1275.661*1.1, _f, _f, _f, _f, _f,
79                           _f, _f, _f, _f, _f, _f, _f, _f,
80                           _f, _f, _f])
```

```
81      psspy.machine_chng_2(5300, r"""2""",
82                           [_i, _i, _i, _i, _i, _i],
83                           [1275.661*1.1, _f, _f, _f, _f, _f,
84                            _f, _f, _f, _f, _f, _f, _f, _f,
85                            _f, _f, _f])
86      # Blafalli
87      psspy.machine_chng_2(6100, r"""1""",
88                           [_i, _i, _i, _i, _i, _i],
89                           [1329.061*1.1, _f, _f, _f, _f, _f,
90                            _f, _f, _f, _f, _f, _f, _f, _f,
91                            _f, _f, _f])
92      psspy.machine_chng_2(6100, r"""2""",
93                           [_i, _i, _i, _i, _i, _i],
94                           [1329.061*1.1, _f, _f, _f, _f, _f,
95                            _f, _f, _f, _f, _f, _f, _f, _f,
96                            _f, _f, _f])
97      psspy.machine_chng_2(6100, r"""3""",
98                           [_i, _i, _i, _i, _i, _i],
99                           [1329.061*1.1, _f, _f, _f, _f, _f,
100                           _f, _f, _f, _f, _f, _f, _f, _f,
101                           _f, _f, _f])
102     psspy.machine_chng_2(6100, r"""4""",
103                          [_i, _i, _i, _i, _i, _i],
104                          [1329.061*1.1, _f, _f, _f, _f, _f,
105                           _f, _f, _f, _f, _f, _f, _f, _f,
106                           _f, _f, _f])
107     psspy.machine_chng_2(6100, r"""5""",
108                          [_i, _i, _i, _i, _i, _i],
109                          [1329.061*1.1, _f, _f, _f, _f, _f,
110                           _f, _f, _f, _f, _f, _f, _f, _f,
111                           _f, _f, _f])
112
113     # Change load in Sweden
114     # Ringfors
115     psspy.load_chng_5(3359, r"""1""",
116                       [_i, _i, _i, _i, _i, _i, _i],
117                       [1460.829*1.15, _f, _f, _f, _f, _f,
118                        _f, _f])
119     psspy.load_chng_5(3359, r"""2""",
120                       [_i, _i, _i, _i, _i, _i, _i],
121                       [1460.829*1.15, _f, _f, _f, _f, _f,
122                        _f, _f])
123     psspy.load_chng_5(3359, r"""3""",
124                       [_i, _i, _i, _i, _i, _i, _i],
125                       [1460.829*1.15, _f, _f, _f, _f, _f,
```

```
126                          _f, _f])
127     psspy.load_chng_5(3359, r"""4""",
128                          [_i, _i, _i, _i, _i, _i, _i],
129                          [1460.829*1.15, _f, _f, _f, _f, _f,
130                           _f, _f])
131
132 if case_2:
133     # Change load in Oslo
134     # Oslo 1
135     psspy.load_chng_5(5400, r"""1""",
136                          [_i, _i, _i, _i, _i, _i, _i],
137                          [1149.765*0.59, _f, _f, _f, _f, _f,
138                           _f, _f])
139     # Oslo 2
140     psspy.load_chng_5(5500, r"""1""",
141                          [_i, _i, _i, _i, _i, _i, _i],
142                          [2203.415*0.59, _f, _f, _f, _f, _f,
143                           _f, _f])
144     psspy.load_chng_5(5500, r"""2""",
145                          [_i, _i, _i, _i, _i, _i, _i],
146                          [2203.415*0.59, _f, _f, _f, _f, _f,
147                           _f, _f])
148
149     # Change production in Sweden
150     # Porjus
151     psspy.machine_chng_2(3115, r"""1""",
152                          [_i, _i, _i, _i, _i, _i],
153                          [1042.0*0.3, _f, _f, _f, _f, _f,
154                           _f, _f, _f, _f, _f, _f, _f, _f,
155                           _f, _f, _f])
156     psspy.machine_chng_2(3115, r"""2""",
157                          [_i, _i, _i, _i, _i, _i],
158                          [1042.0*0.3, _f, _f, _f, _f, _f,
159                           _f, _f, _f, _f, _f, _f, _f, _f,
160                           _f, _f, _f])
161     psspy.machine_chng_2(3115, r"""3""",
162                          [_i, _i, _i, _i, _i, _i],
163                          [1042.0*0.3, _f, _f, _f, _f, _f,
164                           _f, _f, _f, _f, _f, _f, _f, _f,
165                           _f, _f, _f])
166
167 if case_3:
168     # Change production in Finland
169     # Oulu
170     psspy.machine_chng_2(7100, r"""1""",
```

```
171                             [_i, _i, _i, _i, _i, _i],
172                             [715.3333*0.85, _f, _f, _f, _f,
173                              _f, _f, _f, _f, _f, _f, _f, _f,
174                              _f, _f, _f, _f])
175         psspy.machine_chng_2(7100, r"""2""",
176                             [_i, _i, _i, _i, _i, _i],
177                             [715.3333*0.85, _f, _f, _f, _f,
178                              _f, _f, _f, _f, _f, _f, _f, _f,
179                              _f, _f, _f, _f])
180         psspy.machine_chng_2(7100, r"""3""",
181                             [_i, _i, _i, _i, _i, _i],
182                             [715.3333*0.85, _f, _f, _f, _f,
183                              _f, _f, _f, _f, _f, _f, _f, _f,
184                              _f, _f, _f, _f])
185         # Change production in Norway
186         # Blafalli
187         psspy.machine_chng_2(6100, r"""1""",
188                             [_i, _i, _i, _i, _i, _i],
189                             [1329.061*1.1, _f, _f, _f, _f,
190                              _f, _f, _f, _f, _f, _f, _f,
191                              _f, _f, _f, _f, _f])
192         psspy.machine_chng_2(6100, r"""2""",
193                             [_i, _i, _i, _i, _i, _i],
194                             [1329.061*1.1, _f, _f, _f, _f,
195                              _f, _f, _f, _f, _f, _f, _f,
196                              _f, _f, _f, _f, _f])
197         psspy.machine_chng_2(6100, r"""3""",
198                             [_i, _i, _i, _i, _i, _i],
199                             [1329.061*1.1, _f, _f, _f, _f,
200                              _f, _f, _f, _f, _f, _f, _f,
201                              _f, _f, _f, _f, _f])
202         psspy.machine_chng_2(6100, r"""4""",
203                             [_i, _i, _i, _i, _i, _i],
204                             [1329.061*1.1, _f, _f, _f, _f,
205                              _f, _f, _f, _f, _f, _f, _f,
206                              _f, _f, _f, _f, _f])
207         psspy.machine_chng_2(6100, r"""5""",
208                             [_i, _i, _i, _i, _i, _i],
209                             [1329.061*1.1, _f, _f, _f, _f,
210                              _f, _f, _f, _f, _f, _f, _f,
211                              _f, _f, _f, _f, _f])
212
213 if case_4:
214     # Change load in Oslo
215     # Oslo 1
```

```
216     psspy.load_chng_5(5400, r"""1""",
217                       [_i, _i, _i, _i, _i, _i, _i],
218                       [1149.765*1.1, _f, _f, _f, _f, _f,
219                        _f, _f])
220     # Oslo 2
221     psspy.load_chng_5(5500, r"""1""",
222                       [_i, _i, _i, _i, _i, _i, _i],
223                       [2203.415*1.1, _f, _f, _f, _f, _f,
224                        _f, _f])
225     psspy.load_chng_5(5500, r"""2""",
226                       [_i, _i, _i, _i, _i, _i, _i],
227                       [2203.415*1.1, _f, _f, _f, _f, _f,
228                        _f, _f])
229
230     # Change production in Finland
231     # Oulu
232     psspy.machine_chng_2(7100, r"""1""",
233                          [_i, _i, _i, _i, _i, _i],
234                          [715.3333*1.25, _f, _f, _f, _f,
235                           _f, _f, _f, _f, _f, _f, _f, _f,
236                           _f, _f, _f, _f])
237     psspy.machine_chng_2(7100, r"""2""",
238                          [_i, _i, _i, _i, _i, _i],
239                          [715.3333*1.25, _f, _f, _f, _f,
240                           _f, _f, _f, _f, _f, _f, _f, _f,
241                           _f, _f, _f, _f])
242     psspy.machine_chng_2(7100, r"""3""",
243                          [_i, _i, _i, _i, _i, _i],
244                          [715.3333*1.25, _f, _f, _f, _f,
245                           _f, _f, _f, _f, _f, _f, _f, _f,
246                           _f, _f, _f, _f])
247
248 if case_5:
249     # Change load in Oslo
250     # Oslo 1
251     psspy.load_chng_5(5400, r"""1""",
252                       [_i, _i, _i, _i, _i, _i, _i],
253                       [1149.765*0.65, _f, _f, _f, _f,
254                        _f, _f, _f])
255     # Oslo 2
256     psspy.load_chng_5(5500, r"""1""",
257                       [_i, _i, _i, _i, _i, _i, _i],
258                       [2203.415*0.65, _f, _f, _f, _f,
259                        _f, _f, _f])
260     psspy.load_chng_5(5500, r"""2""",
```

```
261                             [_i, _i, _i, _i, _i, _i, _i],
262                             [2203.415*0.65, _f, _f, _f, _f,
263                              _f, _f, _f])
264
265     # Change production in Finland
266     # Oulu
267     psspy.machine_chng_2(7100, r"""1""",
268                             [_i, _i, _i, _i, _i, _i],
269                             [715.3333*0.0, _f, _f, _f,
270                              _f, _f, _f, _f, _f, _f, _f,
271                              _f, _f, _f, _f, _f, _f])
272     psspy.machine_chng_2(7100, r"""2""",
273                             [_i, _i, _i, _i, _i, _i],
274                             [715.3333*0.0, _f, _f, _f, _f,
275                              _f, _f, _f, _f, _f, _f, _f,
276                              _f, _f, _f, _f, _f])
277     psspy.machine_chng_2(7100, r"""3""",
278                             [_i, _i, _i, _i, _i, _i],
279                             [715.3333*0.0, _f, _f, _f, _f,
280                              _f, _f, _f, _f, _f, _f, _f, _f,
281                              _f, _f, _f, _f])
282
283 if case_6:
284     # Change production in Finland
285     # Oulu
286     psspy.machine_chng_2(7100, r"""1""",
287                             [_i, _i, _i, _i, _i, _i],
288                             [715.3333*1.25, _f, _f, _f, _f,
289                              _f, _f, _f, _f, _f, _f, _f, _f,
290                              _f, _f, _f, _f])
291     psspy.machine_chng_2(7100, r"""2""",
292                             [_i, _i, _i, _i, _i, _i],
293                             [715.3333*1.25, _f, _f, _f, _f,
294                              _f, _f, _f, _f, _f, _f, _f, _f,
295                              _f, _f, _f, _f])
296     psspy.machine_chng_2(7100, r"""3""",
297                             [_i, _i, _i, _i, _i, _i],
298                             [715.3333*1.25, _f, _f, _f, _f,
299                              _f, _f, _f, _f, _f, _f, _f, _f,
300                              _f, _f, _f, _f])
301
302     # Change load in Sweden
303     # Ringhals
304     psspy.load_chng_5(3359, r"""1""",
305                             [_i, _i, _i, _i, _i, _i, _i],
```

```
306                         [1460.829*1.1, _f, _f, _f, _f, _f,
307                          _f, _f])
308     psspy.load_chng_5(3359, r"""2""",
309                         [_i, _i, _i, _i, _i, _i, _i],
310                         [1460.829*1.1, _f, _f, _f, _f, _f,
311                          _f, _f])
312     psspy.load_chng_5(3359, r"""3""",
313                         [_i, _i, _i, _i, _i, _i, _i],
314                         [1460.829*1.1, _f, _f, _f, _f, _f,
315                          _f, _f])
316     psspy.load_chng_5(3359, r"""4""",
317                         [_i, _i, _i, _i, _i, _i, _i],
318                         [1460.829*1.1, _f, _f, _f, _f, _f,
319                          _f, _f])
320
321 # Solve the power flow
322 psspy.fnsl([0, 0, 0, 0, 1, 1, 00, 0])
323
324 # Converting the generators
325 psspy.cong(0)
326 # Converting the loads
327 psspy.conl(0, 1, 1, [0, 0], [50.0, 50.0, 0.0, 100.0])
328 psspy.conl(0, 1, 2, [0, 0], [50.0, 50.0, 0.0, 100.0])
329 psspy.conl(0, 1, 3, [0, 0], [50.0, 50.0, 0.0, 100.0])
330
331 # Set the time step for the dynamic simulation
332 psspy.dynamics_solution_params(realar=[_f, _f, 0.005, _f,
333                                        _f, _f, _f, _f])
334
335 i = 1
336 if rotor_angle_stability:
337     for gen_bus in gen_buses:
338         psspy.machine_array_channel([i, 2, gen_bus],
339                                     r"""1""", "")
340         i += 1
341 else:
342     for load_bus in load_buses:
343         if voltage_stability:
344             psspy.voltage_channel([i, -1, -1, load_bus], "")
345         elif frequency_stability:
346             psspy.bus_frequency_channel([i, load_bus])
347         i += 1
348
349 psspy.branch_p_channel([len(load_buses)+1, -1, -1, 5101,
350                         3359], r"""1""", "")
```

```
psspy.branch_p_channel([len(load_buses)+2, -1, -1, 5101,
                        3359], r"""2""", "")

ierr = psspy.strt(outfile=outputfile)  # Tell PSS/E to write
# to output file

# Simulation ------------------------------------------------

if ierr == 0:
    # nprt: number of time steps between writing to screen
    # nplt: number of time steps between writing to output
    # file
    psspy.run(tpause=5, nprt=0, nplt=0)  # run simulation

    if rotor_angle_stability:
        # Branch fault
        psspy.dist_bus_fault(5101, 1, 420.0,
                             [0.0, -0.2E+10])
        psspy.run(0, 5.26, 100, 1, 0)  # Clearing time
        psspy.dist_clear_fault(1)

    # Contingency
    psspy.branch_chng_3(3359, 5101, r"""2""",
                        [0, _i, _i, _i, _i, _i],
                        [_f, _f, _f, _f, _f, _f,
                         _f, _f, _f, _f, _f, _f],
                        [_f, _f, _f, _f, _f, _f,
                         _f, _f, _f, _f, _f, _f], _s)
    psspy.run(tpause=120)  # Pause after 120 seconds
else:
    print(ierr)

# Read the output file
chnf = dyntools.CHNF(outputfile)
# assign the data to variables
sh_ttl, ch_id, ch_data = chnf.get_data()

# Check if voltage/frequency is within valid limit
for i in range(len(load_buses)):
    end = len(ch_data[i+1]) - 1  # last element
    if voltage_stability:
        volt = ch_data[i+1][end]
        if volt <= 0.9 or volt >= 1.1:
            print('Voltage has exceeded the valid limits at '
                  'bus %i.' % (load_buses[i]))
```

```
396             else:
397                 print('Voltage is within the valid limits.')
398         elif frequency_stability:
399             freq = ch_data[i+1][end] + 1
400             if freq <= 0.998 or freq >= 1.002:
401                 print('Frequency has exceeded the valid limits '
402                       'at bus %i.' % (load_buses[i]))
403             else:
404                 print('Frequency is within the valid limits.')
405
406 # Plotting
407 if plotting == 1:
408     if rotor_angle_stability:
409         for i in range(len(gen_buses)):
410             plt.figure(i+1)
411             plt.title('Electric power at bus %i' %
412                       (gen_buses[i]))
413             plt.xlabel('Time [s]')
414             plt.ylabel('Electric power [pu]')
415             plt.plot(ch_data['time'], ch_data[i+1])
416     else:
417         for i in range(len(load_buses)):
418             plt.figure(i+1)
419             if voltage_stability:
420                 plt.title('Voltage at load %i' %
421                           (load_buses[i]))
422                 plt.ylabel('Voltage [pu]')
423             elif frequency_stability:
424                 plt.title('Frequency deviation at load %i'
425                           % (load_buses[i]))
426                 plt.ylabel('Frequency deviation [pu]')
427             plt.xlabel('Time [s]')
428             plt.ylabel('Voltage [pu]')
429             plt.plot(ch_data['time'], ch_data[i+1])
430     plt.show()
431
432 # Plot power flow on Haslesnittet
433 plt.figure(len(load_buses)+1)
434 plt.title('Power flow Hasle - Ringhals, line 1')
435 plt.xlabel('Time [s]')
436 plt.ylabel('Power [MW]')
437 plt.plot(ch_data['time'], ch_data[len(load_buses)+1])
438
439 plt.figure(len(load_buses)+2)
440 plt.title('Power flow Hasle - Ringhals, line 2')
```

```
441 plt.xlabel('Time [s]')
442 plt.ylabel('Power [MW]')
443 plt.plot(ch_data['time'], ch_data[len(load_buses)+2])
444
445 plt.show()
```

D | Model data for the N44 test system

```
%% bus data
%       bus_i    type    Pd      Qd      Gs      Bs      area
Vm      Va       baseKV  zone    Vmax    Vmin
mpc.bus = [
        3000    2       4261.968    1701    0       0       23
0.98639 0.7998  420     1       1.1     0.9;
        3020    1       1219        616     0       0       23
0.9826  0.3674  420     1       1.1     0.9;
        3100    1       621         110     0       0       22
0.96568 8.3321  420     1       1.1     0.9;
        3115    2       621         650     0       0       21
1       35.2503 420     1       1.1     0.9;
        3200    1       0           0       0       0       23
0.97198 2.4758  420     1       1.1     0.9;
        3244    1       0           0       0       0       22
1.00143 8.3711  300     1       1.1     0.9;
        3245    2       0           0       0       0       22
1       8.0285  420     1       1.1     0.9;
        3249    2       2265        650     0       0       21
1       42.3757 420     1       1.1     0.9;
        3300    3       2434.716    800     0       0       23
1       0       420     1       1.1     0.9;
        3359    2       5843.316    2400    0       0       23
0.97417 0.7266  420     1       1.1     0.9;
        3360    1       -330        262     0       0       23
0.97064 1.2058  135     1       1.1     0.9;
        3701    1       0           0       0       0       21
1.01192 40.5938 300     1       1.1     0.9;
        5100    2       1154.17     70      0       0       16
1       8.3386  300     1       1.1     0.9;
        5101    1       0           0       22.3    -974.4  16
```

```
0.98345  9.148    420      1         1.1      0.9;
         5102     1        0            0       0.2      0.1      16
0.98578  14.8182  420      1         1.1      0.9;
         5103     1        0            0       0        0        16
0.98504  15.2817  420      1         1.1      0.9;
         5300     2        2651        -70      0        0        15
1        35.0971  300      1         1.1      0.9;
         5301     1        0            0       0        0        15
0.9936   27.0296  420      1         1.1      0.9;
         5304     1        0            0       0        0        15
0.98801  20.8902  420      1         1.1      0.9;
         5305     1        0            0       0        0        15
0.99511  21.6393  420      1         1.1      0.9;
         5400     2        1149.765    100      0        0        12
1.007    26.417   300      1         1.1      0.9;
         5401     1        0            0       -0.2     -0.5     12
0.99321  21.3852  420      1         1.1      0.9;
         5402     1        0            0       0        0        12
1.0022   26.2509  420      1         1.1      0.9;
         5500     2        4406.83     400      0.3      1.3      11
1.004    5.4597   300      1         1.1      0.9;
         5501     1        0            0       -21.6    974.4    11
1.00245  7.0831   420      1         1.1      0.9;
         5600     2        1349.724    250      0        0        13
1.01     24.8332  300      1         1.1      0.9;
         5601     1        0            0       0        0        13
1.01809  26.1378  300      1         1.1      0.9;
         5602     1        0            0       0        0        13
0.98532  16.1085  420      1         1.1      0.9;
         5603     1        0            0       -0.3     -1.3     13
0.95282  15.0512  300      1         1.1      0.9;
         5610     1        1412        363      0        0        13
0.95049  14.5152  300      1         1.1      0.9;
         5620     1        414         175      0        0        13
1.00896  24.6935  300      1         1.1      0.9;
         5999     2        0            0       0        0        14
1.005    27.83    300      1         1.1      0.9;
         6000     1        0            0       0        0        14
1.005    27.8262  300      1         1.1      0.9;
         6001     1        0            0       0.4      0.4      14
1.00022  26.1887  420      1         1.1      0.9;
         6100     2        2399.51     800      0        0        14
1        53.9795  300      1         1.1      0.9;
         6500     2        3039        999      0        0        17
1        10.4344  300      1         1.1      0.9;
         6700     2        2489        150      0        0        18
1.02     36.3696  300      1         1.1      0.9;
         6701     1        0            0       0        0        18
1.00754  36.2747  420      1         1.1      0.9;
         7000     2        7967.63     350      0        0        32
1        36.5444  420      1         1.1      0.9;
         7010     1        -1219       600      0        0        32
0.99636  36.965   420      1         1.1      0.9;
         7020     1        343         -4       0        0        32
```

```
1.00002  36.4265  420      1        1.1      0.9;
         7100     2        2863.368    400     0       0       31
1        37.4676  420      1        1.1      0.9;
         8500     2        3720        1299    0       0       24
0.96301  -5.8804  420      1        1.1      0.9;
         8600     1        546         10      0       0       24
0.96294  -6.0828  420      1        1.1      0.9;
         8700     1        628         0       0       0       24
0.963    -6.1132  420      1        1.1      0.9;
];

%% generator data
%        bus      Pg       Qg       Qmax     Qmin     Vg       mBase
status   Pmax     Pmin     Pc1      Pc2      Qc1min   Qc1max   Qc2min
Qc2max   ramp_agc ramp_10  ramp_30  ramp_q   apf
mpc.gen = [
         3000     1100        967          967     -967        1
1300        1     1167        0            0 0      0          0
0        0        0        0        0        0        0;
         3000     1100        967          967     -967        1
1300        1     1167        0            0 0      0          0
0        0        0        0        0        0        0;
         3000     0           0            967     -967        1
1300        0     1167        0            0 0      0          0
0        0        0        0        0        0        0;
         3115     1175        437.966      933     -933        1
1450.62     1     1305.56     0            0 0      0          0
0        0        0        0        0        0        0;
         3115     1175        437.966      933     -933        1
1450.62     1     1305.56     0            0 0      0          0
0        0        0        0        0        0        0;
         3115     1175        437.966      933     -933        1
1450.62     1     1305.56     0            0 0      0          0
0        0        0        0        0        0        0;
         3245     1000        653.471      670     -670        1
1234.57     1     1111.11     1110         0 0      0          0
0        0        0        0        0        0        0;
         3249     1042        97.228       986     -986        1
1357        1     1230        0            0 0      0          0
0        0        0        0        0        0        0;
         3249     1042        97.228       986     -986        1
1357        1     1230        0            0 0      0          0
0        0        0        0        0        0        0;
         3249     1042        97.228       986     -986        1
1357        1     1230        0            0 0      0          0
0        0        0        0        0        0        0;
         3249     1042        97.228       986     -986        1
1357        1     1230        0            0 0      0          0
0        0        0        0        0        0        0;
         3249     1042        97.228       986     -986        1
1357        1     1230        0            0 0      0          0
0        0        0        0        0        0        0;
         3249     1042        97.228       986     -986        1
1357        1     1230        0            0 0      0          0
```

```
0       0       0       0       0       0       0;
        3249    1042        97.228      986     -986        1
1357        1   1230        0           0 0       0         0
0       0       0       0       0       0       0;
        3300    998.733     653.676     767     -767        1
1100        1   1000        0           0 0       0         0
0       0       0       0       0       0       0;
        3300    998.733     653.676     767     -767        1
1100        1   1000        0           0 0       0         0
0       0       0       0       0       0       0;
        3300    998.733     653.676     767     -767        1
1100        1   1000        0           0 0       0         0
0       0       0       0       0       0       0;
        3359    1110        983         983     -983        1
1350        1   1217        1216        0 0       0         0
0       0       0       0       0       0       0;
        3359    1100        983         983     -983        1
1350        1   1217        1216        0 0       0         0
0       0       0       0       0       0       0;
        3359    1100        983         983     -983        1
1350        1   1217        1216        0 0       0         0
0       0       0       0       0       0       0;
        3359    0           602.864     983     -983        1
1350        0   1           0           0         0         0
0       0       0       0       0       0       0         0;
        3359    0           602.864     983     -983        1
1350        0   1           0           0 0       0         0
0       0       0       0       0       0       0;
        3359    0           0           983     -983        1
1350        0   1           0           0 0       0         0
0       0       0       0       0       0       0;
        5100    972.437     735.142     850     -850        1
1200        1   1100        1099        0 0       0         0
0       0       0       0       0       0       0;
        5300    1275.661    383.448     850     -850        1
1574.89     1   1417.401    0           0 0       0         0
0       0       0       0       0       0       0;
        5300    1275.661    383.448     850     -850        1
1574.89     1   1417.401    0           0 0       0         0
0       0       0       0       0       0       0;
        5400    1305.328    296.332     900     -900        1.007
1611.516    1   1450.364    0           0         0         0
0       0       0       0       0       0       0         0;
        5400    1305.328    296.332     900     -900        1.007
1611.516    1   1450.364    0           0         0         0
0       0       0       0       0       0       0         0;
        5500    1131.563    81.38       1200      -1200     1.004
1450        1   1280        1279        0 0       0         0
0       0       0       0       0       0       0;
        5600    1245.995    432.931     850     -850        1.01
1538.265    1   1384.438    0           0         0         0
0       0       0       0       0       0       0         0;
        5600    1245.995    432.931     850     -850        1.01
1538.265    1   1384.438    0           0         0         0
```

```
0       0       0       0       0       0       0       0;
        5999    735.73          291.059 500     -500    1.005
896.59      1   817.478         0       0 0       0     0
0       0       0       0       0       0       0;
        6100    1329.061        239.332 900     -900    1
1634.96     1   1476.734        0       0 0       0     0
0       0       0       0       0       0       0;
        6100    1329.061        239.332 900     -900    1
1634.96     1   1476.734        0       0 0       0     0
0       0       0       0       0       0       0;
        6100    1329.061        239.332 900     -900    1
1634.96     1   1476.734        0       0 0       0     0
0       0       0       0       0       0       0;
        6100    1329.061        239.332 900     -900    1
1634.96     1   1476.734        0       0 0       0     0
0       0       0       0       0       0       0;
        6100    1329.061        239.332 900     -900    1
1634.96     1   1476.734.       0       0 0       0     0
0       0       0       0       0       0       0;
        6500    814.333         355.511 800     -800    1
1100        1   1000            999     0 0       0     0
0       0       0       0       0       0       0;
        6500    814.333         355.511 800     -800    1
1100        1   1000            999     0 0       0     0
0       0       0       0       0       0       0;
        6500    814.333         355.511 800     -800    1
1100        1   1000            999     0 0       0     0
0       0       0       0       0       0       0;
        6500    0               0       800     -800    1
1100        0   1               0       0       0       0
0       0       0       0       0       0       0       0;
        6700    1753            99.14   900     -900    1.02
2144.444    1   1930            1929    0 0       0     0
0       0       0       0       0       0       0;
        6700    1753            99.14   900     -900    1.02
2144.444    1   1930            1929    0 0       0     0
0       0       0       0       0       0       0;
        7000    1085.5          158.744 911     -911    1
1278        1   1167            1166    0 0       0     0
0       0       0       0       0       0       0;
        7000    1085.5          158.744 911     -911    1
1278        1   1167            1166    0 0       0     0
0       0       0       0       0       0       0;
        7000    1085.5          158.744 911     -911    1
1278        1   1167            1166    0 0       0     0
0       0       0       0       0       0       0;
        7000    1085.5          158.744 911     -911    1
1278        1   1167            1166    0 0       0     0
0       0       0       0       0       0       0;
        7000    1085.5          158.744 911     -911    1
1278        1   1167            1166    0 0       0     0
```

```
0       0       0       0       0       0       0;
        7000    0           0           911     -911    1
1278        0   1           0           0 0     0       0
0       0       0       0       0       0       0;
        7000    0           0           911     -911    1
1278        0   1           0           0 0     0       0
0       0       0       0       0       0       0;
        7000    0           0           911     -911    1
1278        0   1           0           0 0     0       0
0       0       0       0       0       0       0;
        7100    715.333     113.175     700     -700    1
1000        1   900         0           0 0     0       0
0       0       0       0       0       0       0;
        7100    715.333     113.175     700     -700    1
1000        1   900         0           0 0     0       0
0       0       0       0       0       0       0;
        7100    715.333     113.174     700     -700    1
1000        1   900         0           0 0     0       0
0       0       0       0       0       0       0;
        8500    994         917         917     -917    1.02
1300        1   1183        1182        0 0     0       0
0       0       0       0       0       0       0;
        8500    0           0           917     -917    1.02
1300        0   1           0           0 0     0       0
0       0       0       0       0       0       0;
        8500    0           0           917     -917    1.02
1300        0   1           0           0 0     0       0
0       0       0       0       0       0       0;
        8500    0           0           917     -917    1.02
1300        0   1           0           0 0     0       0
0       0       0       0       0       0       0;
        8500    0           0           917     -917    1.02
1300        0   1           0           0 0     0       0
0       0       0       0       0       0       0;
        8500    0           0           917     -917    1.02
1300        0   1           0           0 0     0       0
0       0       0       0       0       0       0;
];

%% generator cost data
% model startup shutdown    n  c_2  c_1 c0
mpc.gencost = [
    2   0   0   3   0.03  0 0;
    2   0   0   3   0.03  0 0;
    2   0   0   3   0.03  0 0;
    2   0   0   3   0.03  0 0;
    2   0   0   3   0.03  0 0;
    2   0   0   3   0.03  0 0;
    2   0   0   3   0.03  0 0;
    2   0   0   3   0.03  0 0;
    2   0   0   3   0.03  0 0;
    2   0   0   3   0.03  0 0;
    2   0   0   3   0.03  0 0;
    2   0   0   3   0.03  0 0;
    2   0   0   3   0.03  0 0;
    2   0   0   3   0.03  0 0;
```

```
    2    0    0    3    0.03   0 0;
    2    0    0    3    0.03   0 0;
    2    0    0    3    0.03   0 0;
    2    0    0    3    0.03   0 0;
    2    0    0    3    0.03   0 0;
    2    0    0    3    0.03   0 0;
    2    0    0    3    0.03   0 0;
    2    0    0    3    0.03   0 0;
    2    0    0    3    0.03   0 0;
    2    0    0    3    0.03   0 0;
    2    0    0    3    0.01   0 0;
    2    0    0    3    0.01   0 0;
    2    0    0    3    0.01   0 0;
    2    0    0    3    0.01   0 0;
    2    0    0    3    0.01   0 0;
    2    0    0    3    0.01   0 0;
    2    0    0    3    0.01   0 0;
    2    0    0    3    0.01   0 0;
    2    0    0    3    0.01   0 0;
    2    0    0    3    0.01   0 0;
    2    0    0    3    0.01   0 0;
    2    0    0    3    0.01   0 0;
    2    0    0    3    0.01   0 0;
    2    0    0    3    0.01   0 0;
    2    0    0    3    0.01   0 0;
    2    0    0    3    0.01   0 0;
    2    0    0    3    0.01   0 0;
    2    0    0    3    0.01   0 0;
    2    0    0    3    0.01   0 0;
    2    0    0    3    0.01   0 0;
    2    0    0    3    0.01   0 0;
    2    0    0    3    0.01   0 0;
    2    0    0    3    0.01   0 0;
    2    0    0    3    0.01   0 0;
    2    0    0    3    0.01   0 0;
    2    0    0    3    0.01   0 0;
    2    0    0    3    0.01   0 0;
    2    0    0    3    0.01   0 0;
    2    0    0    3    0.01   0 0;
    2    0    0    3    0.01   0 0;
    2    0    0    3    0.01   0 0;
    2    0    0    3    0.01   0 0;
    2    0    0    3    0.01   0 0;
    2    0    0    3    0.01   0 0;
    2    0    0    3    0.01   0 0;
    2    0    0    3    0.01   0 0;
    2    0    0    3    0.01   0 0;
    2    0    0    3    0.01   0 0;
    2    0    0    3    0.01   0 0;
];

%% branch data
%       fbus     tbus     r        x        b    rateA rateB    rateC
ratio    angle    status   angmin   angmax
```

```
mpc.branch = [
        3000    3020    -0      0.006   0       0       0       0
0       0       1       -360    360;
        3000    3115    0.045   0.54    0.5     0       0       0
        0       0       1       -360    360;
        3000    3245    0.0048  0.072   0.05    0       0       0
        0       0       1       -360    360;
        3000    3245    0.0108  0.12    0.05    0       0       0
        0       0       1       -360    360;
        3000    3300    0.0036  0.048   0.03    0       0       0
        0       0       1       -360    360;
        3000    3300    0.0054  0.06    0.025   0       0       0
        0       0       1       -360    360;
        3100    3115    0.018   0.24    0.11    0       0       0
        0       0       1       -360    360;
        3100    3200    0.024   0.144   0.2     0       0       0
        0       0       1       -360    360;
        3100    3200    0.024   0.144   0.2     0       0       0
        0       0       1       -360    360;
        3100    3200    0.024   0.144   0.2     0       0       0
        0       0       1       -360    360;
        3100    3249    0.018   0.258   0.16    0       0       0
        0       0       1       -360    360;
        3100    3359    0.048   0.3     0.25    0       0       0
        0       0       1       -360    360;
        3100    3359    0.024   0.138   0.24    0       0       0
        0       0       1       -360    360;
        3115    3245    0.027   0.3     0.14    0       0       0
        0       0       1       -360    360;
        3115    3249    0.009   0.12    0.08    0       0       0
        0       0       1       -360    360;
        3115    6701    0.024   0.24    0.1     0       0       0
        0       0       1       -360    360;
        3115    7100    0.024   0.078   0.13    0       0       0
        0       0       1       -360    360;
        3200    3300    0.012   0.12    0.06    0       0       0
        0       0       1       -360    360;
        3200    3359    0.006   0.12    0.07    0       0       0
        0       0       1       -360    360;
        3200    8500    0.006   0.102   0.06    0       0       0
        0       0       1       -360    360;
        3244    6500    0.006   0.12    0.06    0       0       0
        0       0       1       -360    360;
        3249    7100    0.012   0.045   0.078   0       0       0
        0       0       1       -360    360;
        3300    8500    0.012   0.138   0.06    0       0       0
        0       0       1       -360    360;
        3300    8500    0.0072  0.162   0.1     0       0       0
        0       0       1       -360    360;
        3359    5101    0.0096  0.156   0.09    1200    1200
1200    0       0       1       -360    360;
        3359    5101    0.012   0.132   0.06    0       0       0
        0       0       0       -360    360; %contingency on this
line
```

```
        3359    8500    0.0072  0.162   0.1     0       0       0
        0       0       1       -360    360;
        3359    8500    0.015   0.192   0.09    0       0       0
        0       0       1       -360    360;
        3701    6700    0.15    1.2     0.03    0       0       0
0       0       1       -360    360;
        5100    5500    0.0162  0.156   0.044   0       0       0
0       0       1       -360    360;
        5100    6500    0.048   0.54    0.06    0       0       0
0       0       1       -360    360;
        5101    5102    0.0048  0.06    0.09    0       0       0
        0       0       1       -360    360;
        5101    5103    0.006   0.084   0.04    0       0       0
        0       0       1       -360    360;
        5101    5501    0.006   0.09    0.55    0       0       0
        0       0       1       -360    360;
        5102    5103    0.0024  0.042   0.03    0       0       0
        0       0       1       -360    360;
        5102    5304    0.0102  0.144   0.07    0       0       0
        0       0       1       -360    360;
        5102    6001    0.018   0.276   0.13    0       0       0
        0       0       1       -360    360;
        5103    5304    0.012   0.15    0.07    0       0       0
        0       0       1       -360    360;
        5103    5304    0.0078  0.12    0.06    0       0       0
        0       0       1       -360    360;
        5300    6100    0.0126  0.132   0.01    0       0       0
0       0       1       -360    360;
        5301    5304    0.006   0.12    0.06    0       0       0
        0       0       1       -360    360;
        5301    5305    0.0042  0.072   0.031   0       0       0
        0       0       1       -360    360;
        5301    6001    0.0078  0.12    0.05    0       0       0
        0       0       1       -360    360;
        5304    5305    0.006   0.09    0.05    0       0       0
        0       0       1       -360    360;
        5304    5305    0.0078  0.0102  0.04    0       0       0
        0       0       1       -360    360;
        5400    5500    0.0054  0.564   0.05    0       0       0
0       0       1       -360    360;
        5400    6000    0.0198  0.216   0.025   0       0       0
0       0       1       -360    360;
        5401    5501    0.0105  0.162   0.08    0       0       0
        0       0       1       -360    360;
        5401    5602    0.0096  0.153   0.09    0       0       0
        0       0       1       -360    360;
        5401    6001    0.00384 0.06    0.028   0       0       0
        0       0       1       -360    360;
        5402    6001    0.00042 0.006   0.003   0       0       0
        0       0       1       -360    360;
        5500    5603    0.03    0.36    0.05    0       0       0
0       0       1       -360    360;
        5600    5601    0.018   0.204   0.02    0       0       0
0       0       1       -360    360;
```

```
        5600    5603    0.012   0.132   0.02    0       0       0
        0       0       1       -360    360;
        5600    5620    -0      0.006   0       0       0       0
0       0       1       -360    360;
        5600    6000    0.012   0.12    0.07    0       0       0
        0       0       1       -360    360;
        5603    5610    -0      0.006   0       0       0       0
0       0       1       -360    360;
        5999    6000    -0      0.0001  0       0       0       0
0       0       1       -360    360;
        6000    6100    0.0204  0.252   0.03    0       0       0
0       0       1       -360    360;
        6500    6700    0.102   1.08    0.1     0       0       0
0       0       1       -360    360;
        6500    6700    0.06    0.78    0.12    0       0       0
        0       0       1       -360    360;
        7000    7010    -0      0.006   0       0       0       0
0       0       1       -360    360;
        7000    7020    -0      0.006   0       0       0       0
0       0       1       -360    360;
        7000    7100    0.024   0.072   0.13    0       0       0
        0       0       1       -360    360;
        7000    7100    0.024   0.072   0.13    0       0       0
        0       0       1       -360    360;
        7000    7100    0.024   0.084   0.13    0       0       0
        0       0       1       -360    360;
        8500    8600    -0      0.006   0       0       0       0
0       0       1       -360    360;
        8500    8700    -0      0.006   0       0       0       0
0       0       1       -360    360;
        3244    3245    0.005   0.02    0       0       0       0
1       0       1       -360    360;
        3701    3249    0.02    0.5     0       0       0       0
1       0       1       -360    360;
        3359    3360    0.005   0.02    0       0       0       0
        0.9998  0       1       -360    360;
        5101    5100    0.0008  0.0305  0       0       0       0
        1.00635 0       1       -360    360;
        5300    5301    0.0016  0.061   0       0       0       0
        1       0       1       -360    360;
        5400    5401    0.0032  0.12    0       0       0       0
        1.00635 0       1       -360    360;
        5400    5402    0.0004  0.015   0       0       0       0
        1       0       1       -360    360;
        5500    5501    0.0004  0.015   0       0       0       0
        1.0126  0       1       -360    360;
        5601    6001    0.0002  0.0076  0       0       0       0
        1.01806 0       1       -360    360;
        5603    5602    0.0008  0.0305  0       0       0       0
        0.96825 0       1       -360    360;
        6000    6001    0.0004  0.015   0       0       0       0
        1.00625 0       1       -360    360;
        6700    6701    0.005   0.02    0       0       0       0
        1.0125  0       1       -360    360;
```

```
];

%% bus names
mpc.bus_name = {
         '            ';
         '            ';
         '            ';
         '            ';
         '            ';
         '            ';
         '            ';
         '            ';
         '            ';
         '            ';
         '            ';
         '            ';
         '            ';
         '            ';
         '            ';
         '            ';
         '            ';
         '            ';
         '            ';
         '            ';
         '            ';
         '            ';
         '            ';
         '            ';
         '            ';
         '            ';
         '            ';
         '            ';
         '            ';
         '            ';
         '            ';
         '            ';
         '            ';
         '            ';
         '            ';
         '            ';
         '            ';
         '            ';
         '            ';
         '            ';
         '            ';
         '            ';
         '            ';
         '            ';
         '            ';
};
```

Margrete Haaland

Stability limits for optimal power flow related to congestion management

NTNU
Norwegian University of
Science and Technology